Edith Cowan University

Research Online

Research outputs 2022 to 2026

1-1-2023

Methane emissions in seagrass meadows as a small offset to carbon sequestration

Yvonne Y. Y. Yau

Gloria Reithmaier

Caludia Majtényi-Hill

Oscar Serrano
Edith Cowan University

Nerea Piñeiro-Juncal

See next page for additional authors

Follow this and additional works at: https://ro.ecu.edu.au/ecuworks2022-2026

 Part of the Environmental Sciences Commons, Marine Biology Commons, and the Oceanography Commons

10.1029/2022JG007295

Yau, Y. Y. Y., Reithmaier, G., Majtényi-Hill, C., Serrano, O., Piñeiro-Juncal, N., Dahl, M., . . . Santos, I. R. (2023). Methane emissions in seagrass meadows as a small offset to carbon sequestration. JGR Biogeosciences, 128(6), article e2022JG007295. https://doi.org/10.1029/2022JG007295

This Journal Article is posted at Research Online.
https://ro.ecu.edu.au/ecuworks2022-2026/2880

Authors

Yvonne Y. Y. Yau, Gloria Reithmaier, Caludia Majtényi-Hill, Oscar Serrano, Nerea Piñeiro-Juncal, Martin Dahl, Miguel A. Mateo, Stefano Bonaglia, and Isaac R. Santos

This journal article is available at Research Online: https://ro.ecu.edu.au/ecuworks2022-2026/2880

Check for updates

JGR Biogeosciences

RESEARCH ARTICLE
10.1029/2022JG007295

Methane Emissions in Seagrass Meadows as a Small Offset to Carbon Sequestration

Yvonne Y. Y. Yau[1], Gloria Reithmaier[1], Claudia Majtényi-Hill[1], Oscar Serrano[2,3], Nerea Piñeiro-Juncal[2,4,5], Martin Dahl[2,6], Miguel Angel Mateo[2,3], Stefano Bonaglia[1], and Isaac R. Santos[1]

[1]Department of Marine Sciences, University of Gothenburg, Gothenburg, Sweden, [2]Centro de Estudios Avanzados de Blanes, Consejo Superior de Investigaciones Científicas, Blanes, Spain, [3]School of Science and Centre for Marine Ecosystems Research, Edith Cowan University, Joondalup, WA, Australia, [4]Department of Biology & CESAM—Centre for Environmental and Marine Studies, University of Aveiro, Aveiro, Portugal, [5]Facultade de Bioloxía, CRETUS, EcoPast (GI-1553), Universidade de Santiago de Compostela, Santiago de Compostela, Spain, [6]School of Natural Sciences, Technology and Environmental Studies, Södertörn University, Huddinge, Sweden

Key Points:

- High-resolution CH_4 observations reveal diel cycles linked to seagrass photosynthesis
- Dense seagrass meadow had lower sea-air CH_4 flux than the area with patchy and dead seagrass
- CH_4 emissions were a small offset to seagrass C sequestration on local and global scales

Correspondence to:

Y. Y. Y. Yau,
yvonne.yau@gu.se

Citation:

Yau, Y. Y. Y., Reithmaier, G., Majtényi-Hill, C., Serrano, O., Piñeiro-Juncal, N., Dahl, M., et al. (2023). Methane emissions in seagrass meadows as a small offset to carbon sequestration. *Journal of Geophysical Research: Biogeosciences*, *128*, e2022JG007295. https://doi.org/10.1029/2022JG007295

Received 12 DEC 2022
Accepted 6 MAY 2023

Author Contributions:

Conceptualization: Yvonne Y. Y. Yau, Claudia Majtényi-Hill, Oscar Serrano, Nerea Piñeiro-Juncal, Miguel Angel Mateo, Stefano Bonaglia, Isaac R. Santos
Data curation: Gloria Reithmaier, Claudia Majtényi-Hill, Oscar Serrano, Nerea Piñeiro-Juncal, Martin Dahl, Miguel Angel Mateo, Stefano Bonaglia, Isaac R. Santos
Formal analysis: Yvonne Y. Y. Yau, Stefano Bonaglia
Funding acquisition: Oscar Serrano, Isaac R. Santos
Investigation: Gloria Reithmaier, Claudia Majtényi-Hill, Martin Dahl, Stefano Bonaglia
Methodology: Yvonne Y. Y. Yau, Gloria Reithmaier, Claudia Majtényi-Hill, Oscar Serrano, Nerea Piñeiro-Juncal, Miguel Angel Mateo, Stefano Bonaglia, Isaac R. Santos

© 2023 The Authors.
This is an open access article under the terms of the Creative Commons Attribution-NonCommercial License, which permits use, distribution and reproduction in any medium, provided the original work is properly cited and is not used for commercial purposes.

Abstract Seagrass meadows are effective carbon sinks due to high primary production and sequestration in sediments. However, methane (CH_4) emissions can partially counteract their carbon sink capacity. Here, we measured diffusive sediment-water and sea-air CO_2 and CH_4 fluxes in a coastal embayment dominated by *Posidonia oceanica* in the Mediterranean Sea. High-resolution timeseries observations revealed large spatial and temporal variability in CH_4 concentrations (2–36 nM). Lower sea-air CH_4 emissions were observed in an area with dense seagrass meadows compared to patchy seagrass. A 6%–40% decrease of CH_4 concentration in the surface water around noon indicates that photosynthesis likely limits CH_4 fluxes. Sediments were the major CH_4 source as implied from radon (a natural porewater tracer) observations and evidence for methanogenesis in deeper sediments. CH_4 sediment-water fluxes (0.1 ± 0.1–0.4 ± 0.1 μmol m^{-2} d^{-1}) were higher than average sea-air CH_4 emissions (0.12 ± 0.10 μmol m^{-2} d^{-1}), suggesting that dilution and CH_4 oxidation in the water column could reduce net CH_4 fluxes into the atmosphere. Overall, relatively low sea-air CH_4 fluxes likely represent the net emissions from subtidal seagrass habitat not influenced by allochthonous CH_4 sources. The local CH_4 emissions in *P. oceanica* can offset less than 1% of the carbon burial in sediments (142 ± 69 g CO_{2eq} m^{-2} yr^{-1}). Combining our results with earlier observations in other seagrass meadows worldwide reveals that global CH_4 emissions only offset a small fraction (<2%) of carbon sequestration in sediments from seagrass meadows.

Plain Language Summary Seagrass meadows are hotspots for marine carbon storage in sediments. Part of the sediment carbon can be released as carbon dioxide and methane (CH_4). Methane has 45–96 times more powerful global warming effect than carbon dioxide. If seagrass meadows release CH_4, the emissions counteract their climate mitigation potential. We measured greenhouse gas concentrations and fluxes in a seagrass-dominated Mediterranean embayment. Low CH_4 coincided with oxygen produced from seagrass photosynthesis. Areas with dense seagrass meadows had lower CH_4 emissions. Overall, seagrass-dominated coasts were a small source of CH_4 that offset only <2% of carbon buried in sediments on local and global scales. Hence, seagrass meadows remain an effective carbon sink.

1. Introduction

Seagrass meadows are effective carbon sinks recognized for their potential role in climate change mitigation (Fourqurean et al., 2012; Lovelock & Duarte, 2019; Mcleod et al., 2011). Seagrass meadows sequester carbon dioxide (CO_2) through photosynthesis (Van Dam et al., 2021) and trap allochthonous particles within their canopy (Gacia et al., 2002). Part of this carbon is then stored as biomass and as organic carbon in sediments for centuries and even millennia (Serrano et al., 2021, 2016). Seagrass meadows account for 10%–18% of the total carbon burial (27 44 Tg C yr^{-1}) in the ocean, even though they cover only 0.1% of the global ocean area (Kennedy et al., 2010). In addition, about 5% of the particulate organic carbon and dissolved organic carbon produced within seagrass habitats is exported beyond the meadows and stored in the deep ocean (Duarte & Krause-Jensen, 2017). Seagrass meadows are considered an important blue carbon ecosystem that should be protected and restored to mitigate anthropogenic CO_2 emissions.

Resources: Yvonne Y. Y. Yau, Claudia Majtényi-Hill, Oscar Serrano, Nerea Piñeiro-Juncal, Miguel Angel Mateo, Stefano Bonaglia, Isaac R. Santos
Supervision: Gloria Reithmaier, Claudia Majtényi-Hill, Oscar Serrano, Miguel Angel Mateo, Stefano Bonaglia, Isaac R. Santos
Validation: Claudia Majtényi-Hill, Oscar Serrano, Isaac R. Santos
Visualization: Yvonne Y. Y. Yau, Claudia Majtényi-Hill, Nerea Piñeiro-Juncal
Writing – original draft: Yvonne Y. Y. Yau
Writing – review & editing: Gloria Reithmaier, Claudia Majtényi-Hill, Oscar Serrano, Nerea Piñeiro-Juncal, Martin Dahl, Miguel Angel Mateo, Stefano Bonaglia, Isaac R. Santos

Posidonia oceanica is the dominant seagrass species along the Mediterranean coast and an important blue carbon ecosystem (Telesca et al., 2015). *P. oceanica* is a slow-growing and long-living seagrass, which accumulates 84 ± 20 g C m^{-2} yr^{-1} of organic carbon in the sediment (Serrano et al., 2016). Due to their slow decay rates and recalcitrant nature, *P. oceanica* is one of the largest blue carbon sinks among seagrass species (Gacia et al., 2002; Kaal et al., 2018; Serrano et al., 2018). A special feature of *P. oceanica* is the formation of thick (up to 6.5 m) and old (up to millennia) organic detritus known as *mattes*, storing large quantities of organic matter in the sediments (Lo Iacono et al., 2008; Mateo et al., 1997). These dead mattes can remain as important carbon and biogeochemical sinks even 30 yr after seagrass death of the meadow (Apostolaki et al., 2022). However, natural and human disturbances such as moorings and coastal development destroy seagrass meadows potentially leading to reduction of carbon stocks and increased emissions of CO_2 and CH_4 to the atmosphere (Carnell et al., 2020; Lyimo et al., 2018).

The coastal ocean is a hotspot of CH_4 emissions, contributing 75% of the global oceanic CH_4 emissions (Weber et al., 2019). In marine waters, CH_4 is mainly produced in sediments during anaerobic microbial degradation of organic carbon via methanogenesis (Martens & Klump, 1980). It usually occurs after all the other energetically favorable electron acceptors become depleted in sediments (Froelich et al., 1979). Thus, oxygen, nitrate, metal oxide and sulfate availability in marine sediments can limit methanogenesis and CH_4 emissions (Egger et al., 2016a). Seagrass meadows' large and deep organic carbon storage can create conditions for organic matter degradation CH_4 production. The presence of methylated compounds in seagrass rhizosphere provides another pathway for CH_4 production, even in dead seagrass meadows (Schorn et al., 2022). The net CH_4 emission is also controlled by production and oxidation in sediment and water column before reaching the atmosphere (Egger et al., 2016b; Ward et al., 1987). Understanding both sediment-water and sea-air fluxes can provide insight on net CH_4 fluxes to the atmosphere.

Since CH_4 is a potent greenhouse gas with 45–96 times greater sustained-flux global warming potential (SGWP) than CO_2, on a mass basis (Neubauer & Megonigal, 2015), CH_4 emissions can offset some of the carbon sequestered in sediments. Although measurements of CH_4 fluxes have been widely performed in mangroves (Call et al., 2019), saltmarshes (Yau et al., 2022), and other coastal ecosystems (Borges & Abril, 2011), CH_4 fluxes in seagrass meadows remain poorly constrained across multiple spatial and temporal scales. The sea-air and sediment-water CH_4 fluxes from seagrass ranged from 0 to 400 μmol m^{-2} d^{-1}, resulting in global upscaled fluxes of 0.18 Tg CH_4 per year (Al-Haj et al., 2022). Several seagrass meadow CH_4 flux estimates considered sediment-water fluxes, obtained from benthic chambers and sediment incubation approaches, to be equivalent to sea-air fluxes. This assumes that sediment CH_4 propagates through the shallow water column and reaches the atmosphere unmodified.

Here, we report high-resolution timeseries observations of dissolved CH_4 over multiple diel cycles and estimate sediment-water and sea-air CH_4 fluxes in *P. oceanica* meadows at a Mediterranean bay. We quantified sea-air CO_2 and CH_4 fluxes above the seagrass using automated, in situ surface water observations (including radon (^{222}Rn) measurements, a natural porewater tracer), and at the sediment-water interface using sediment cores. This study aims to (a) estimate sea-air and sediment-water CH_4 fluxes, (b) evaluate the spatial and diel variability of sea-air CH_4 fluxes, (c) examine whether CH_4 emissions can partially offset carbon sequestration in seagrass on both local and global scales.

2. Materials and Methods

2.1. Sampling Location

Field observations were performed at Portlligat Bay (42°17'32" N, 3°7'28" E) on the northeast coast of Spain in the Mediterranean Sea. The bay is shallow ranging from 2 to 10 m, with <0.5 m tidal ranges (Serrano et al., 2012). *P. oceanica* is the dominant seagrass species in the bay, covering 41% of the area (0.12 km^2). The seabed is irregular with mounds of matte deposits (ranging from 3.5 to 6 m in thickness) formed by *P. oceanica* debris intertwined with fine to medium sands (Lo Iacono et al., 2008). Dense *P. oceanica* (>600 shoots m^{-2}) were found at the center and north of the bay, whereas patchy seagrass meadows with sand and dead mattes were found at the south of the bay (Figure 1). The presence of dead matte is due to the loss of seagrass canopy and the exposure of underground plant organs such as root, rhizome, and sheath remains of *P. oceanica*. The seagrass area at the south side of the bay is quite patchy, with dead matte a few meters away from living seagrass. We observed that there are no living seagrass remains in the dead matte area.

21698961, 2023, 6, Downloaded from https://agupubs.onlinelibrary.wiley.com/doi/10.1029/2022JG007295 by Edith Cowan University, Wiley Online Library on [22/08/2023]. See the Terms and Conditions (https://onlinelibrary.wiley.com/terms-and-conditions) on Wiley Online Library for rules of use; OA articles are governed by the applicable Creative Commons License

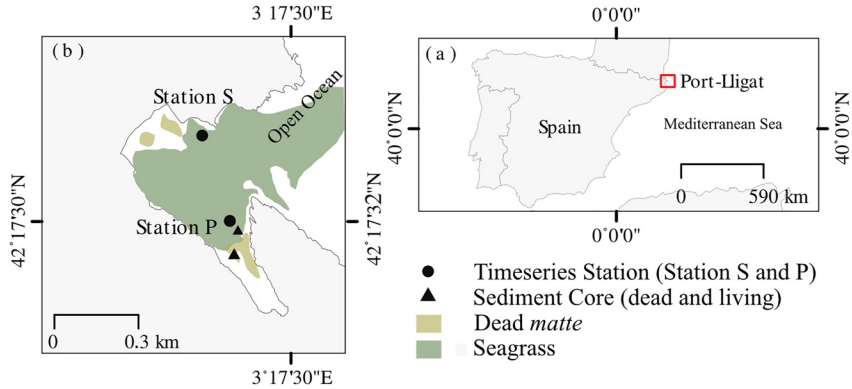

Figure 1. Study site map. (a) Location of Portlligat bay; (b) Portlligat bay with location of timeseries Stations S and P, sediment core of living and dead seagrasses, extent of *Posidonia oceanica* meadows (shaded green) modified from Leiva-Dueñas et al. (2018), and the dead *matte* (shaded brown).

Anthropogenic disturbances in the embayment are limited to boating and the deployment of environmentally friendly moorings in the center of the bay. An ephemeral stream is located at the northeast edge of the bay, but there are no permanent rivers supplying freshwater to the bay.

2.2. Timeseries and Spatial Survey

Two timeseries stations were deployed simultaneously during 11–18 September 2021 (Figure 1). Station S was in a healthy seagrass-dominated area (42°17'38" N, 3°17'19 E"), whilst Station P was surrounded by patchy seagrass meadows, including dead seagrass areas (42°17'29" N, 3°17'22 E"). Station S was located at northeast of the bay, ~180 m off the shore and Station P was at the southern inner corner of the bay (~90 m off the shore). Precipitation events were recorded from 01:00 to 09:00 on 16 September with a maximum 2.9 cm hr^{-1}.

Water depth, salinity, and temperature were measured every 5 min (Levelogger 5 LTC, Solinst), whereas dissolved oxygen (DO) was recorded at 1 min intervals (miniDOT, PME), which were installed close to the sediment surface. Radon was measured with a ^{222}Rn-air analyzer (RAD7), while CO_2 and CH_4 were measured with a greenhouse gas analyzer (LI-7810, LI-COR). Both were connected to a Durridge shower head gas exchange device as described elsewhere (Webb et al., 2016 and references there in). A water pump was attached at the side of the boat (~50 cm deep) to sample surface water at 3 L min^{-1} to the showerhead gas exchange. There were data gaps in the patchy seagrass due to instrument failure (days 13 and 14 September 2021). We did not fill the gaps due to the complex relationship of CO_2 and CH_4 with other environmental parameters such as oxygen and light. CO_2 and CH_4 concentrations were recorded at 1 s intervals and radon at 30 min intervals. Time lags of 30, 10, and 30 min were applied to ^{222}Rn, CO_2, and CH_4 respectively to account for gas equilibrium between water and the closed air loop (Webb et al., 2016). The data were aggregated into 5 min intervals.

A spatial survey was conducted to measure ^{222}Rn, CO_2, and CH_4 continuously across the bay covering a track of 1.5 km on 18 September 2021 from 16:00 to 17:30 using the same experimental setup as described above. The survey was conducted using a kayak with an average speed of less than 2 km per hr, generating minimum disturbance. Average CH_4 fluxes for the whole bay area were estimated using inverse distance weighted interpolation methods. Solubility of CO_2 and CH_4 was calculated as a function of temperature and salinity using Weiss (1974) and Yamamoto et al. (1976), respectively, and normalized to the Schmidt number as described in Wanninkhof (2014). Meteorological parameters such as radiation, wind speed and precipitation were obtained from the nearest automated station of Roses (42° 16' 20.56" N, 3° 11' 1.16" E) from the government of Catalonia.

2.3. Sediment and Porewater Analysis

Six sediment cores were collected by manual hammering of PVC pipes (1 m long and 60 mm inner diameter) in both dead and living seagrass (Figure 1) through SCUBA diving. Although the dead and living seagrass sediment cores were collected near Station P, they were collected in the middle of distinct patches of dead matte and living seagrass with >30 m^2 area.

21698961, 2023, 6, Downloaded from https://agupubs.onlinelibrary.wiley.com/doi/10.1029/2022JG007295 by Edith Cowan University, Wiley Online Library on [22/08/2023]. See the Terms and Conditions (https://onlinelibrary.wiley.com/terms-and-conditions) on Wiley Online Library for rules of use; OA articles are governed by the applicable Creative Commons License

21698961, 2023, 6, Downloaded from https://agupubs.onlinelibrary.wiley.com/doi/10.1029/2022JG007295 by Edith Cowan University, Wiley Online Library on [22/08/2023]. See the Terms and Conditions (https://onlinelibrary.wiley.com/terms-and-conditions) on Wiley Online Library for rules of use; OA articles are governed by the applicable Creative Commons License

To sample for dissolved CH_4 in porewater, a push-core with pre-drilled holes (1 cm diameter) was used to minimize the oxidation during sampling. We extracted 3 mL of wet sediment using a cut-off plastic syringe and transferred into 22 mL gas-tight vials containing 10 mL of a 1M NaOH solution to preserve methane. The vials were then crimped immediately using aluminum caps with butyl rubber stoppers. Back in the lab, all headspace (7–10 mL) were transferred into a second N_2 flushed vial using a gas-tight syringe. The headspace CH_4 concentrations were then measured using a gas chromatographer (Thermo Scientific Trace 1300) equipped with flame ionization detector. Reference gas standards of 1.9 and 50 ppm (Air Liquide Gas AB) were used for instrument calibration. The porewater CH_4 concentrations were calculated from the measured headspace concentrations (Hoehler et al., 2000; Equation 1):

$$[CH_4] = \frac{P * V_H}{R * T * \varnothing * V_S} \quad (1)$$

where $[CH_4]$ is the porewater CH_4 concentration (nM), P is the methane partial pressure inside the vial (atm), V_H and V_S are the volume of headspace in each vial and the sediment sample (mL), R is the universal gas constant (L atm K^{-1} mol^{-1}), T is the laboratory temperature (°C) and $\varnothing$ is the sediments porosity in each sediment layer. Sediment porosity was calculated from water content (weight difference of wet and dry sample weight after drying at 100°C) and sediment bulk density (Lengier et al., 2021).

Porewater for DIC was extracted from sediment cores using Rhizon samplers (Rhizosphere research product). Approximately 10–15 mL of porewater was collected. DIC samples were collected in 12 mL Exetainers without headspace. DIC concentrations were analyzed by total dissolved inorganic carbon analyzer (Appollo AS-C5) at the University of Gothenburg. Certified reference material (Dickson Laboratory, Scripps Institute of Oceanography) was used as the standard. The analytical precision was 2% for porewater.

The organic matter content of the sediment layers was estimated based on the Loss of Ignition method, after homogenizing the samples with a mill and combusting for 4 hr at 500°C (Heiri et al., 2001).

2.4. Estimation of Sediment-Water and Sea-Air CH_4 and CO_2 Fluxes

^{222}Rn was used as a qualitative tracer for benthic exchange in this study. Porewater observations, including estimates of ^{222}Rn diffusion from sediments, bay water residence times, and radium (^{226}Ra) observations would be needed to build a full radon mass balance (Adyasari et al., 2023) and quantify related porewater benthic CH_4 fluxes. Unfortunately, these additional ^{226}Ra data are not available because sampling large volumes of porewater is often required for ^{222}Rn analysis, which was not possible in the organic rich matte (Lee & Kim, 2006). Hence, CH_4 sediment-water fluxes were calculated using Fick's law and ^{222}Rn observations are used to qualitatively support Fick's law interpretations. The sediment-water CO_2 and CH_4 diffusive fluxes were calculated using Fick's first law:

$$J = -\varnothing D_S \frac{dC}{dz} \quad (2)$$

where J is diffusive flux of CH_4 and DIC (μmol m^{-2} d^{-1}), $\varnothing$ is the sediment porosity, D_S is the sediment diffusion coefficient (cm^2 s^{-1}), C is the CH_4 concentration in porewater (μM) and z is the sediment depth (cm). The values of $\frac{dC}{dz}$ were obtained from the slope of the linear regressions where $p < 0.05$. The diffusion in sediment (D_S) was adjusted to the diffusion in seawater using sediment tortuosity (θ) based on $D_S = \frac{D_{SW}}{\theta}$, where the seawater diffusion coefficient (D_{SW}) for CH_4 and DIC seawater at 20°C was 1.39×10^{-9} and 9.89×10^{-10} (Lerman, 1979). θ was calculated from sediment porosity using $\theta = 1 - \ln(\varnothing^2)$ (Boudreau, 1997; Lengier et al., 2021).

The sea-air CO_2 and CH_4 fluxes were determined by gradient of sea-air gas concentration, gas solubility and gas transfer velocity (Equation 1).

$$FCH_4 / FCO_2 = k\, k_0 (P_W - P_a) \quad (3)$$

where F is the CO_2 and CH_4 flux (mmol m^{-2} d^{-1}), k represents gas transfer velocity (m d^{-1}), k_0 is the solubility coefficient (mol kg^{-1} atm^{-1}), and P_w and Pa are the partial pressures (μatm) of CO_2 and CH_4 in water and air, respectively. The atmospheric partial pressures of CO_2 and CH_4 were 419 and 1.9 ppm, respectively. Positive sea-air gas flux values indicate gas evasion from water to air. Four empirical models were used to determine the gas transfer velocity k, which was based on the water depth and wind speed at 10 m above sea level (m s^{-1}) (Borges et al., 2004; Dobashi & Ho, 2022; Raymond & Cole, 2001; Wanninkhof, 2014; Table 1). These models

21698961, 2023, 6, Downloaded from https://agupubs.onlinelibrary.wiley.com/doi/10.1029/2022JG007295 by Edith Cowan University, Wiley Online Library on [22/08/2023]. See the Terms and Conditions (https://onlinelibrary.wiley.com/terms-and-conditions) on Wiley Online Library for rules of use; OA articles are governed by the applicable Creative Commons License

Table 1
Models for Gas Transfer Velocity Parameterizations

Model	Parameters	Location	Equation
Raymond and Cole (2001)	Wind speed	River and estuary	$k_{600} = 1.91e^{0.35u_{10}}$
Borges et al. (2004)	Wind speed	Estuary	$k_{600} = 5.141{u_{10}}^{0.758}$
Wanninkhof (2014) [a]	Wind speed	River	$k_{660} = 0.251{u_{10}}^{2}$
Dobashi and Ho (2022)	Wind speed	Seagrass	$k_{600} = 0.143{u_{10}}^{2}$

Note. k is normalized to Schmidt number (k_{600}) as a function of temperature and salinity. u_{10} is the wind speed at 10 m height (m s^{-1}).
[a]k_{660} is converted to k_{600} for comparison by assuming that both the Schmidt number had the same ratio and exponent of −0.5.

were selected for intermediate wind speed of 3–15 m s^{-1}. The Dobashi and Ho (2022) model was determined from seagrass meadows in Florida Bay, which accounted for the wave resistance by seagrass and lower wind fetch in meadows. We chose Dobashi and Ho (2022) model for further analysis and upscaling as it is more suitable for our coastal bay and prevents overestimation of fluxes.

CH_4 flux estimates were converted to CO_2 equivalents based on the SGWP 96 and 45 for time horizons of 20 and 100 yr, respectively (Al-Haj & Fulweiler, 2020; Neubauer & Megonigal, 2015). This is used to describe the greenhouse budget over a defined time horizon. The CO_2 equivalent emissions of CH_4 were calculated as follows:

$$\mathrm{SGWP}_{100/20}\left(\mathrm{Tg\,CO}_{2-\mathrm{eq}}\right) = \mathrm{FCH}_4 * f * 365 * A * \mathrm{SGWP}_{100/20} * \quad (4)$$

where FCH_4 represents average CH_4 flux (μmol m^{-2} d^{-1}); A is the area of seagrass (km^2), SGWP of 100 and 20 yr of 45 and 96, f is the conversion factor from μmol to Tg.

To investigate whether CO_2 and CH_4 fluxes were different between stations, Mann–Whitney tests were used due to the non-normal distributed data. Spearman's Rank-order test was used to determine the correlations between different environmental parameters. All statistical tests were considered significant when $p < 0.05$.

3. Results

3.1. Timeseries Observations

The average water temperature and salinity were similar at Stations S and P, with 23.3°C ± 0.7°C (SD) and 36 ± 1 respectively (Figure 2). The water depth ranged from 1.4 to 2.4 m and wind speeds at 10 m above sea level averaged 2.1 ± 1.6 m s^{-1} over the study period. The light intensity underwater during daytime was higher in Station P (1,747 ± 633 lum ft^{-2}) than Station S (1,044 ± 670 lum ft^{-2}). Average DO saturation at both Stations S and P was undersaturated (78% ± 16.0% and 75% ± 18%, respectively). DO followed the expected diel pattern with oversaturated and undersaturated conditions during noon and night, respectively (Figure 3). The daytime average wind speed, and the CH_4 and CO_2 fluxes were mostly higher than at nighttime (Table 2). pCO_2 exhibited a diel cycle with a peak around 9–10 a.m. and lowest values around 6 p.m. in Station S. pCO_2 was negatively correlated with DO in both stations (Figure 3). The hourly average CH_4 concentrations were significantly different at both sites, with Station P being five times higher than Station S. We observed a 40% decrease in CH_4 concentrations from 13:00 to 16:00 at Station P, but only 5% decrease during 11:00–16:00 in Station S. The hourly average of pCO_2 and CH_4 exhibited a clockwise hysteresis loop with DO saturation at both sites and Station S exhibited a weak but significant correlation between DO saturation and CH_4 (Figure 7). The hourly average CH_4 concentration had a hysteretic pattern to light intensity in Station S but a strong positive correlation in Station P (Figure 7). However, ^{222}Rn did not follow a diel pattern at both stations. While the DO, depth and salinity data during this timeseries were used in a companion paper to estimate primary productivity (Majtényi-Hill et al., 2023), the CO_2, CH_4, and ^{222}Rn data sets are original.

3.2. Spatial Variation

pCO_2 and CH_4 were significantly different between the two stations (Figure 6). pCO_2 values at Station S (538 ± 50 μatm), which is surrounded by healthy seagrass meadows and located further off shore, were lower than at Station P (632 ± 103 μatm), which is mostly surrounded by dead *matte* and organic matter debris over sand and closer to land (Table 2). Similarly, the CH_4 concentrations were three times lower in Station S (2.68 ± 0.17 nM) compared to Station P (8.57 ± 6.72 nM). ^{222}Rn concentration at Station P (377 ± 129 dpm m^3) was also two times

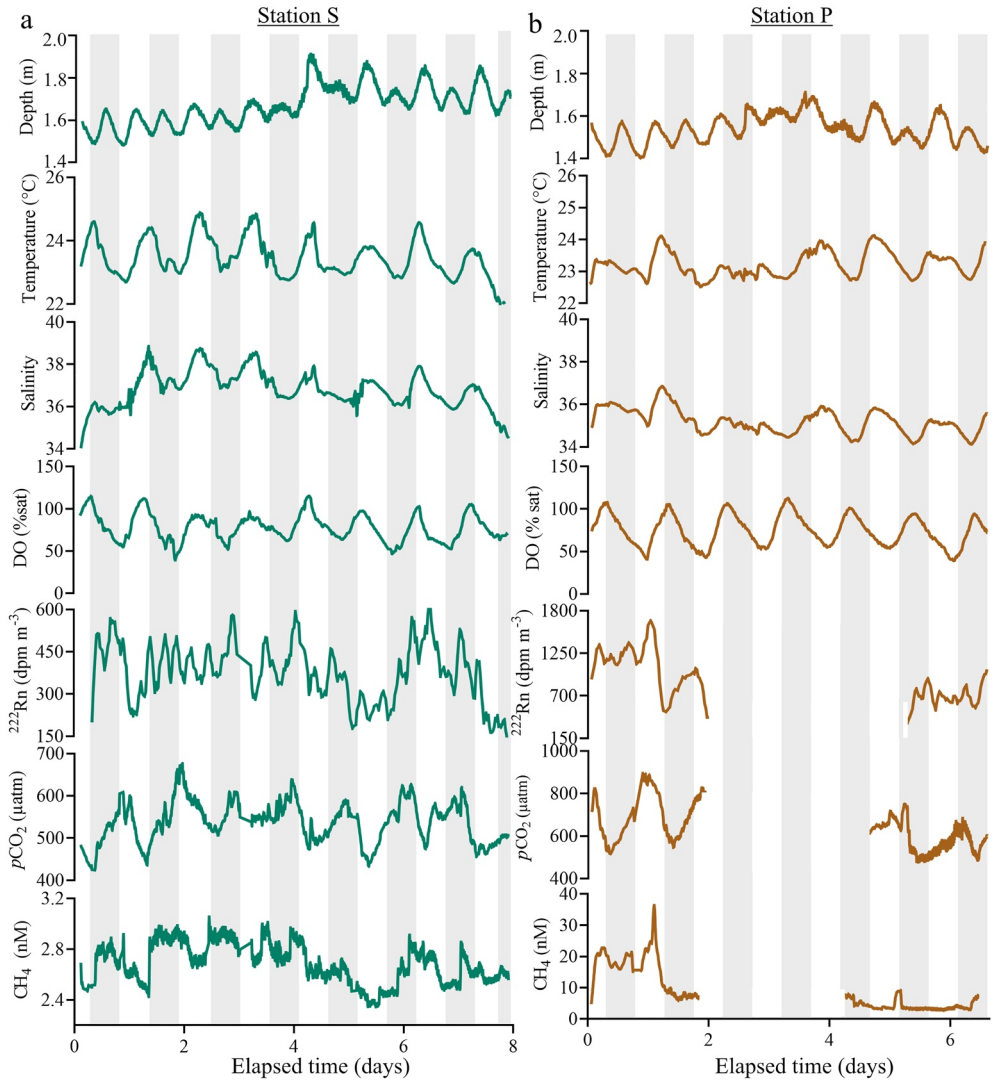

Figure 2. Timeseries observations of dissolved greenhouse gases and ancillary parameters at (a) Station S; and (b) Station P. The shaded area indicates nighttime, whereas the non-shaded area indicates daytime. Gaps in the data were due to instrument failure.

lower than Station S (892 ± 331 dpm m^3) (Figure 2). The high CH_4 concentrations at Station P (peak at 36.3 nM at 13:00) occurred in the first two days of observations coinciding with the high concentrations of ^{222}Rn (peak at 1,886 dpm m^3) and high irradiance (6,000 lum ft^{-2}) (Figure 3). ^{222}Rn concentrations were positively correlated with CH_4 at Station P ($r = 0.73$) and Station S ($r = 0.51$) and pCO_2 ($r = 0.49$ and $r = 0.32$, respectively) (Figure 6).

The CH_4 and CO_2 emissions were calculated from four different gas transfer models. CH_4 emissions estimated by Dobashi and Ho (2022) were 5 times, 10 times, and 2 times lower than those obtained with the other gas transfer models tested: Borges et al. (2004), Raymond and Cole (2001), and Wanninkhof (2014), respectively. Net CH_4 emissions were observed at both stations, with one order of magnitude higher CH_4 sea-air fluxes at Station P (1.25 ± 2.60 µmol m^{-2} d^{-1}) compared to Station S (0.11 ± 0.14 µmol m^{-2} d^{-1}) over the study period. Similarly, net release of CO_2 to the atmosphere was up to 2-fold lower in Station S (0.69 ± 0.91 mmol m^{-2} d^{-1}) compared to Station P (1.1 ± 1.84 mmol m^{-2} d^{-1}).

3.3. Spatial Survey in the Bay

The 2-hr survey across the bay was conducted in late afternoon with wind speed (1.6 m s^{-1}) lower than the average timeseries measurements (2.2 m s^{-1}). CH_4 concentrations varied across the bay, ranging from 2.6 to 6.9 nM.

21698961, 2023, 6, Downloaded from https://agupubs.onlinelibrary.wiley.com/doi/10.1029/2022JG007295 by Edith Cowan University, Wiley Online Library on [22/08/2023]. See the Terms and Conditions (https://onlinelibrary.wiley.com/terms-and-conditions) on Wiley Online Library for rules of use; OA articles are governed by the applicable Creative Commons License

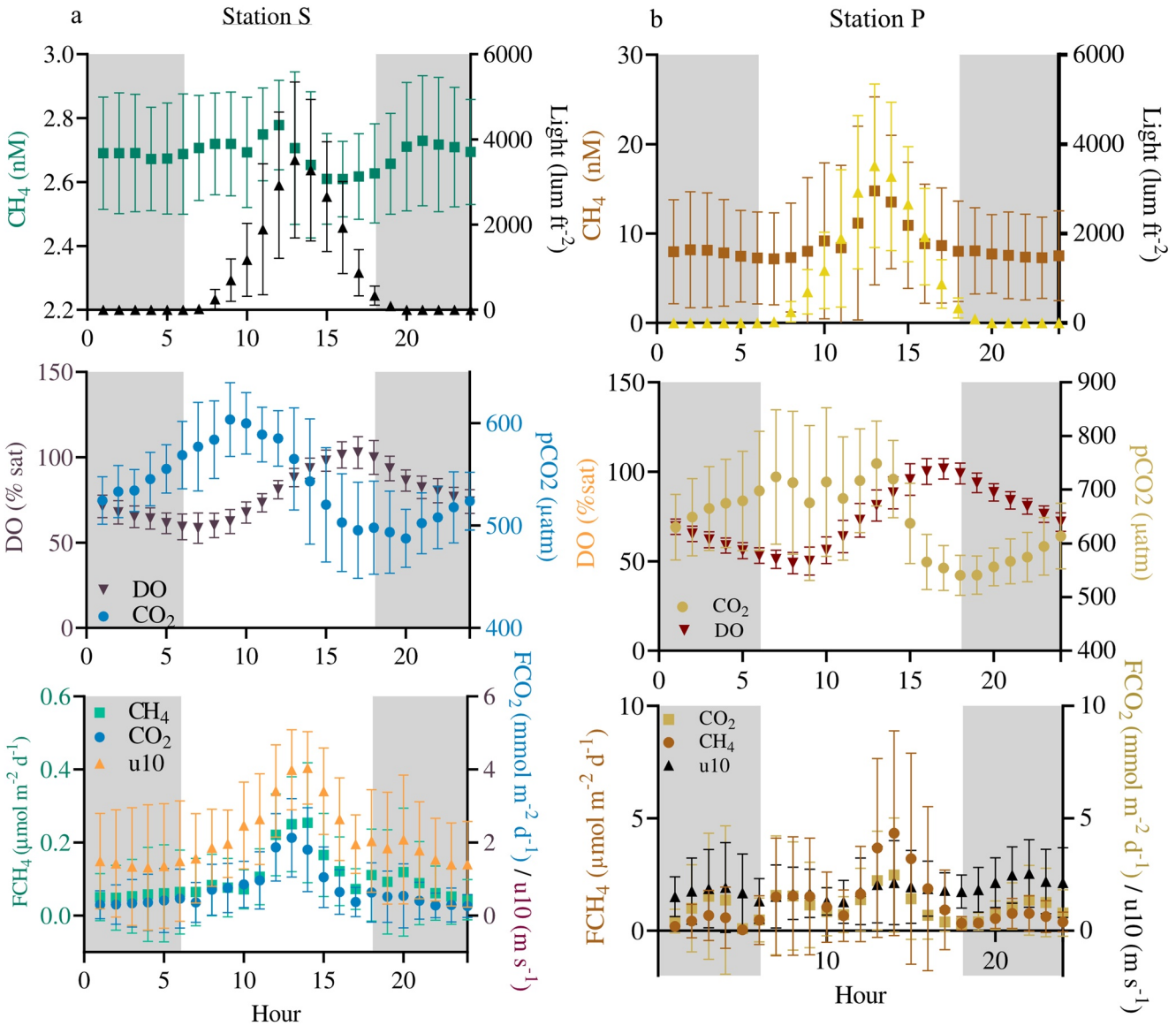

Figure 3. Mean ± standard deviation of hourly concentration of CH_4 (nM), CO_2 (pCO_2), light intensity (lum ft^{-2}), percentage saturation of dissolved oxygen (DO, % sat), wind speed at 10 m above sea level (u10), CO_2 fluxes (FCO_2), and CH_4 fluxes (FCH_4) at (a) Station S and (b) Station P over the period of study. Both CO_2 and CH_4 fluxes were obtained based on the gas transfer model from Dobashi and Ho (2022). The shaded area indicates nighttime, whereas the non-shaded area indicates daytime.

The highest CH_4 concentration was detected around Station P and along the SW shoreline, and further decreased toward the east and the opening toward the Mediterranean Sea (Figure 4). This trend is consistent with timeseries observations where Station P is higher than Station S. Overall, a net release of CH_4 was estimated for the whole bay, ranging from 0.12 ± 0.10 to 2.97 ± 1.47 µmol m^{-2} d^{-1}, depending on the gas transfer model used. The spatial survey represents the average of whole bay (0.21 km^2), which was 50% higher than the average timeseries measurements recorded at Station S and 91% lower at Station P. For the upscaling of CH_4 emissions, we used the average CH_4 flux for the whole bay to account for the spatial differences.

3.4. Porewater Profiles

Sediment cores in both living and dead seagrass areas had similar water content ranging from 40% to 55%. Total organic matter content of sediments was similar between cores from living and dead seagrass areas, with an average of 16.9% and 17.5%, respectively (Table 3). Porewater CH_4 concentration in living seagrass cores (0.4–4.6 µM)

21698961, 2023, 6, Downloaded from https://agupubs.onlinelibrary.wiley.com/doi/10.1029/2022JG007295 by Edith Cowan University, Wiley Online Library on [22/08/2023]. See the Terms and Conditions (https://onlinelibrary.wiley.com/terms-and-conditions) on Wiley Online Library for rules of use; OA articles are governed by the applicable Creative Commons License

21698961, 2023, 6, Downloaded from https://agupubs.onlinelibrary.wiley.com/doi/10.1029/2022JG007295 by Edith Cowan University, Wiley Online Library on [22/08/2023]. See the Terms and Conditions (https://onlinelibrary.wiley.com/terms-and-conditions) on Wiley Online Library for rules of use; OA articles are governed by the applicable Creative Commons License

Table 2
A Summary of Environmental Parameters and GHG Fluxes Measured Simultaneously at Station S and Station P

		Station S			Station P			Spatial survey
Unit		Overall	Day	Night	Overall	Day	Night	Overall
Description		*P.oceanica* dominated			Pachy and dead *P.oceanica*			Whole bay
No. of hours	hr	205	97	108	109	61	48	2
Temperature	°C	23.5 ± 0.6	23.0 ± 0.4	23.0 ± 0.3	23.2 ± 0.4	23.1 ± 0.1	23.3 ± 0.1	23.7
Salinity		36.8 ± 0.9	37 ± 1	37 ± 1	36 ± 1	35 ± 0	35 ± 0	37 ± 0
Water depth	m	1.7 ± 0.1	1.7 ± 1	1.7 ± 1	1.5 ± 0.1	1.5 ± 0.1	1.5 ± 0.1	1.7
Wind speed	$m\ s^{-1}$	2.6 ± 1.6	2.6 ± 1.2	1.6 ± 1.5	1.8 ± 1.4	1.7 ± 0.4	1.9 ± 0.4	1.6 ± 0.1
Irradiance	$lum\ ft^{-2}$	526 ± 942	1,044 ± 670	18 ± 0	873 ± 1,456	1,747 ± 633	33 ± 70	/
DO	% Sat	78 ± 16	80 ± 7	75 ± 6.5	75 ± 18	74 ± 2	73 ± 1	102 ± 1
DO	$mg\ L^{-1}$	5.4 ± 1.1	5.5 ± 0.5	5.2 ± 0.5	5.0 ± 1.3	4.6 ± 0.5	5.6 ± 0.3	7 ± 0
pCO_2	µatm	538 ± 50	556 ± 40	520 ± 28	632 ± 103	668 ± 37	614 ± 20	606 ± 51
CH_4	nM	2.68 ± 0.17	2.68 ± 0.15	2.69 ± 0.18	8.57 ± 6.72	9.48 ± 1.88	7.74 ± 0.74	4.07 ± 1.18
^{222}Rn	$dpm\ m^{-3}$	377 ± 129	386 ± 120	383 ± 131	892 ± 331	863 ± 128	946 ± 85	/
CO_2 flux								
R&C	$mmol\ m^{-2}\ d^{-1}$	3.75 ± 2.63	4.96 ± 2.33	2.71 ± 1.65	6.32 ± 5.59	7.36 ± 2.46	5.71 ± 2.74	4.21 ± 0.84
B04	$mmol\ m^{-2}\ d^{-1}$	7.22 ± 5.27	10.03 ± 4.55	4.72 ± 3.09	11.85 ± 11.05	14.16 ± 5.25	10.22 ± 3.38	9.52 ± 2.01
W14	$mmol\ m^{-2}\ d^{-1}$	1.35 ± 1.78	2.04 ± 1.6	0.77 ± 1.23	2.13 ± 3.58	2.47 ± 1.68	1.91 ± 2.12	0.85 ± 0.20
RY22	$mmol\ m^{-2}\ d^{-1}$	0.69 ± 0.91	1.04 ± 0.81	0.4 ± 0.65	1.1 ± 1.84	1.28 ± 0.87	0.97 ± 1.07	0.38 ± 0.09
CH_4 flux								
R&C	$\mu mol\ m^{-2}\ d^{-1}$	0.56 ± 0.37	0.64 ± 0.31	0.48 ± 0.32	6.59 ± 9.21	8.76 ± 3.87	4.33 ± 0.8	1.33 ± 0.65
B04	$\mu mol\ m^{-2}\ d^{-1}$	1.07 ± 0.71	1.26 ± 0.57	0.83 ± 0.58	12.37 ± 18.18	17.91 ± 7.61	7.62 ± 1.48	2.97 ± 1.47
W14	$\mu mol\ m^{-2}\ d^{-1}$	0.20 ± 0.26	0.27 ± 0.21	0.14 ± 0.22	2.34 ± 4.88	3.72 ± 2.91	1.04 ± 0.85	0.27 ± 0.14
RY22	$\mu mol\ m^{-2}\ d^{-1}$	0.11 ± 0.14	0.14 ± 0.11	0.08 ± 0.12	1.25 ± 2.6	1.98 ± 1.53	0.55 ± 0.44	0.12 ± 0.10

Note. Day indicates data from 06:00 to 18:00 and night indicates data from 18:00 to 06:00. All data are reported as mean ± SD. The sea-air CO_2 and CH_4 fluxes were calculated from four gas transfer velocity models (R&C from Raymond and Cole (2001); B04 from Borges et al. (2004), W14 from Wanninkhof (2014); and RY22 from Dobashi and Ho (2022)).

were two times higher than in the dead seagrass (0.4–2.1 µM). Both cores showed similar CH_4 depth profiles, increasing from 1 µM at the surface up to 6 µM at 50 cm (Figure 5). The estimated sediment diffusive CH_4 flux in living seagrass (0.1–0.4 $\mu mol\ m^{-2}\ d^{-1}$) was 2–11 times higher than in dead seagrass (0–0.1 $\mu mol\ m^{-2}\ d^{-1}$). CH_4 sediment-water fluxes in the living seagrass were two times higher than CH_4 sea-air emissions in the Station S (i.e., seagrass-dominated site), whereas sediment-water CH_4 fluxes in the dead seagrass were 10 times lower than sea-air emissions in Station P (i.e., a mix of patchy and dead seagrass). Porewater DIC concentrations in living seagrass (1,460–8,060 µM) were also two times higher than in the dead seagrass (940–5,390 µM) (Table 3). DIC concentration in dead seagrass remained relatively constant with increasing sediment depth, whilst in living seagrass, DIC increased with depth, with the steepest increase from 0 to 30 cm, where the rhizosphere ends, and then after continued to increase until 70 cm depth (Figure 5). The estimated DIC diffusive flux in the living seagrass (185–355 $\mu mol\ m^{-2}\ d^{-1}$) was three times higher than in the dead seagrass (68–88 $\mu mol\ m^{-2}\ d^{-1}$).

4. Discussion

4.1. Sediment-Water CH_4 Fluxes

Porewater CH_4 concentrations (0.3–2.1 µM) in both living and dead seagrass sediment are similar to those estimated for *Zostera noltii* in France (2.5–8 µM; Deborde et al., 2010), but 20 times higher than those observed in *Posidonia* meadows in Italy (0.04–0.09 µM; Schorn et al., 2022). This difference might be related to abiotic factors including sediment grain-size distribution (i.e., mud content), and/or the quality and quantity of organic carbon in

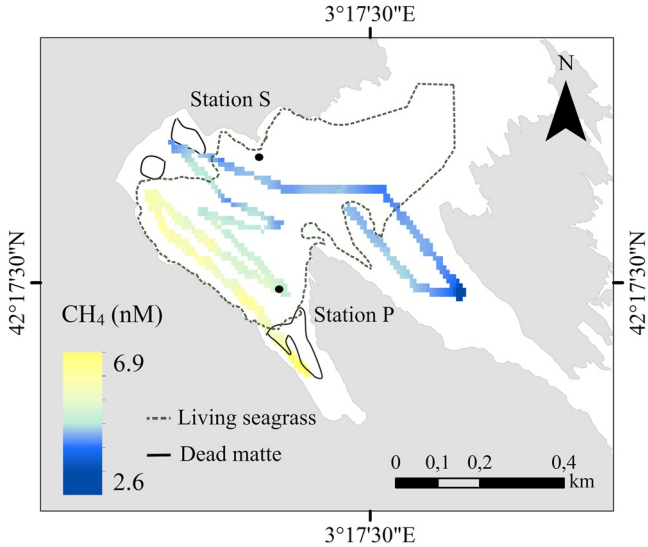

Figure 4. The distribution of CH_4 concentration across Portlligat bay. The track line represents the spatial survey and the color represents the CH_4 concentration. The northeast exit of the bay is the Mediterranean Sea. CO_2 observations during the same survey are reported in a companion paper (Majtényi-Hill et al., 2023).

sediment. Positive correlations between the porewater tracer ^{222}Rn and CH_4 concentrations also suggested that the sediments underlying the seagrasses are the main source of CH_4 (and ^{222}Rn) to the environment (Figure 6). There are no other major ^{222}Rn sources such as fresh groundwater or river water input to the bay.

The living seagrass had a higher CH_4 sediment-water flux than dead seagrass. This seems to be counterintuitive, but living seagrass sediments may host different microbial communities than the dead seagrass sediments (Piñeiro-Juncal et al., 2021, 2018), which can explain differences in CH_4 production. The living seagrass sediment core showed CH_4 production below 40–50 cm, which match depths reached by *P. oceanica* rhizosphere of 43 cm in average (Duarte et al., 2005). This could be related to methylotrophic production of methane associated with seagrass rhizomes as shown before (Schorn et al., 2022). A positive relationship between porewater DIC and CH_4 concentrations suggested that methanogenesis supports organic carbon mineralization (Aleksandra & Katarzyna, 2018). The contribution of methanogenesis to total carbon mineralization was at maximum 0.03%, based on the porewater CH_4: DIC. Both porewater DIC and CH_4 diffusive rates in the living seagrass were 2–3 times higher than in sediments of dead seagrasses, suggesting that living seagrass releases organic carbon together with oxygen in root exudates, which enhances carbon remineralization rates and DIC fluxes (L. Li, 2021). Therefore, living seagrasses, with a higher liable content of organic carbon compared to dead *matte* could stimulate the CH_4 production (Piñeiro-Juncal et al., 2021). This was also observed in sediments with *Z. noltii*, which had four times higher fluxes than bare sediments (Bahlmann et al., 2015). Additional porewater and stable isotope analyses may be needed to interpret the mechanisms of CH_4 production within sediments of living and dead seagrass meadows.

4.2. Diel Pattern in Sea-Air Fluxes of CH_4

A diel sea-air CH_4 pattern with a decreasing trend in the afternoon in both sites suggests that oxygen availability could control CH_4 concentrations (Figure 3). First, we observed a 6%–40% decrease of sea-air CH_4 concentrations in the afternoon coinciding with increasing DO and light intensity, implying a link between peak photosynthesis and the decrease of CH_4. Second, the hysteresis pattern between CH_4, oxygen saturation, and temperature in the dense seagrass site indicates that higher oxygen concentration derived from seagrass photosynthesis could reduce CH_4 fluxes during the afternoon (13:00–17:00; Bahlmann et al., 2015). Similarly, Lyimo et al. (2018) reported that a reduction of photosynthetic activity can result in an increase of CH_4 benthic fluxes in a tropical seagrass meadow. Third, the hysteresis relationship between CH_4 and temperature has also been observed in global wetlands (Chang et al., 2020). Primary productivity could either increase or decrease CH_4 fluxes in freshwater wetlands (Knox et al., 2021; Whiting & Chanton, 1993), yet clear relationships were not observed at the two seagrass meadow stations studied, probably because we had a maximum temperature range of only 1.5°C (Figure 7). The diel CH_4 variation likely implied that the photosynthesis from seagrass drives the oxidation rate of CH_4, controlling CH_4 emissions.

Table 3
Sediment Characteristics and Porewater DIC and CH_4 Concentrations in Cores From Living Meadows and Dead Matte Cores

	Unit	Living	Dead
Dry bulk density[a]	g cm^{-3}	0.2 ± 0.1	0.3 ± 0.1
Water content[a]	%	51 ± 5.1	46 ± 4.9
Particulate organic matter[a]	%	16.9 ± 7.4	17.5 ± 7.4
DIC	μM	4,094 ± 1,827	2,974 ± 939
CH_4	μM	2.3 ± 1.5	1.1 ± 0.6
CH_4 sediment-water flux	μmol m^{-2} d^{-1}	0.25 ± 0.1	0.1 ± 0.1
DIC sediment-water flux	μmol m^{-2} d^{-1}	280 ± 87	78 ± 15

Note. All data are reported as mean ± SD.
[a]Average of the first 50 cm of the sediment.

4.3. Spatial Pattern in Sea-Air Fluxes of CH_4

The patchy seagrass meadows contributed to a ten times higher sea-air CH_4 flux than the dense seagrass, which could be attributed to the presence of dead seagrass, less oxidation ability, CH_4 production from epiphytes and differences in microbial activities (Hilt et al., 2022). Dense seagrass exhibited a hysteresis correlation between DO% and CH_4, whereas there is no clear relationship in patchy seagrass (Figure 7). This indicates that oxygen in dense seagrass could promote higher oxidation, controlling the CH_4 fluxes. Moreover, patchy seagrass sites exhibited a more pronounced CH_4 peak during

21698961, 2023, 6, Downloaded from https://agupubs.onlinelibrary.wiley.com/doi/10.1029/2022JG007295 by Edith Cowan University, Wiley Online Library on [22/08/2023]. See the Terms and Conditions (https://onlinelibrary.wiley.com/terms-and-conditions) on Wiley Online Library for rules of use; OA articles are governed by the applicable Creative Commons License

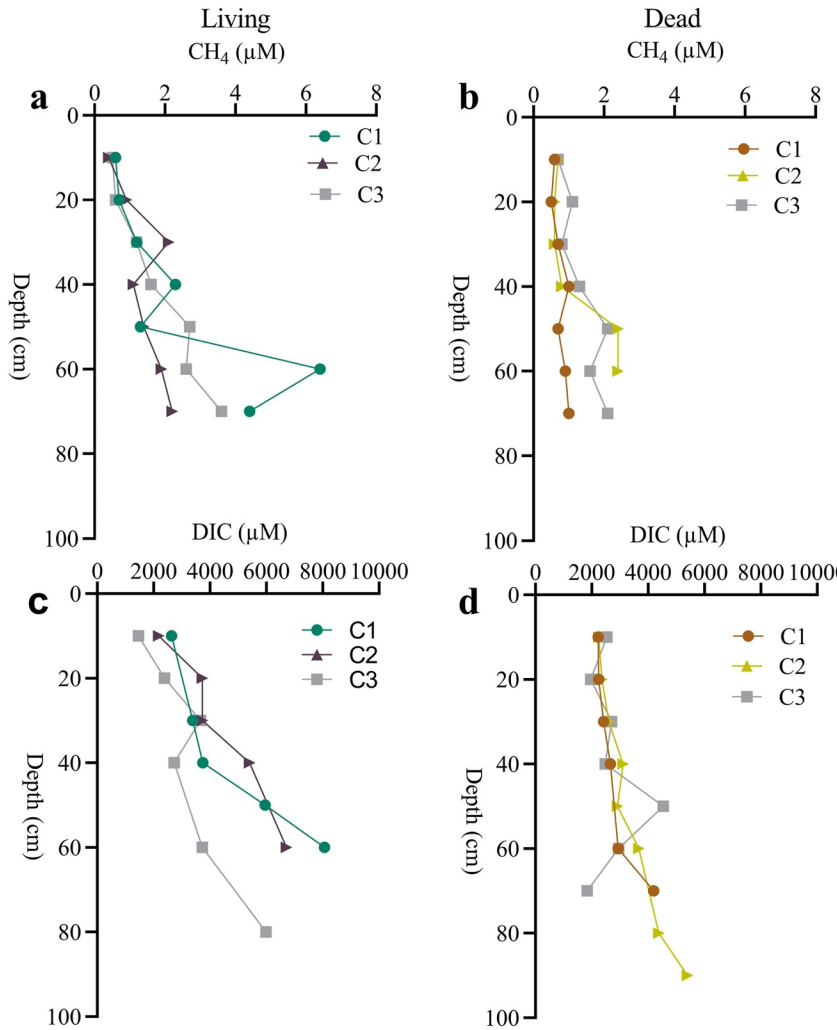

Figure 5. Vertical sediment profiles of porewater CH_4 and DIC concentrations (μM) in three replicate cores within (a, c) living meadows and (b, d) dead matte.

noon, which was not observed in the dense seagrass. This pattern was also observed in other submerged vegetated habitats such as a temperate freshwater marsh in China and a mixed-vegetated habitat in the Baltic Sea during summer (Ding et al., 2004; Roth et al., 2022). We cannot exclude that the positive correlation of light intensity with CH_4 concentrations, only observed in patchy seagrass, could be related to abiotic CH_4 photoproduction (Hilt et al., 2022; Y. Li et al., 2020) or, more likely, to light inhibition of methane oxidation in surface water (Murase & Sugimoto, 2005; Sieczko et al., 2020) (Figure 7). More studies are needed to understand the contribution of both seagrass meadows and dead *matte* habitat to sea-air CH_4 fluxes.

The spatial differences in CH_4 concentrations could link to the proximity to the open ocean. The patchy seagrass area had two times higher ^{222}Rn concentrations than the area with dense seagrass. As the dense seagrass site was closer to the open ocean, ocean waters could dilute CH_4 concentration within the area, resulting in a lower CH_4 and ^{222}Rn concentrations compared to the more enclosed location of Station P with patchy seagrass (Rosentreter et al., 2021). Moreover, higher sediment-water fluxes than the sea-air fluxes in dense seagrass (Station S) might imply that the sediment could be the main CH_4 source. However, for the patchy seagrass, an opposite trend was observed with lower sediment-water fluxes than the sea-air fluxes, implying some extra CH_4 production in the dead seagrass sites such as groundwater or horizontal transport of CH_4 within the bay.

21698961, 2023, 6, Downloaded from https://agupubs.onlinelibrary.wiley.com/doi/10.1029/2022JG007295 by Edith Cowan University, Wiley Online Library on [22/08/2023]. See the Terms and Conditions (https://onlinelibrary.wiley.com/terms-and-conditions) on Wiley Online Library for rules of use; OA articles are governed by the applicable Creative Commons License

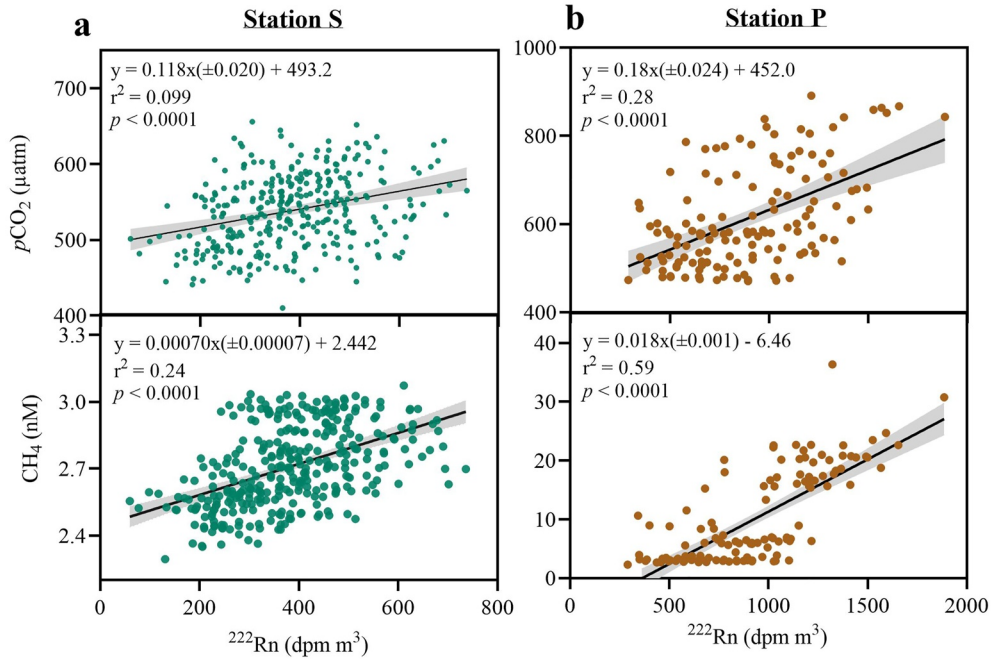

Figure 6. Scatter plot of ^{222}Rn against CH_4 and pCO_2 in Station S (a) and Station P (b). The solid line represents the fitted regression equation, the shaded area is the 95% confidence limits of the regression line, the r^2 value and p-value indicates the degree of correlation, and the significance.

4.4. Low Seagrass CH_4 Emissions on Local and Global Scales

The average sea-air CH_4 flux (0.12 ± 0.10 µmol CH_4 m^{-2} d^{-1}) estimated is the lowest among seagrass meadows reported to date, where the maximum can reach up to 307 µmol CH_4 m^{-2} d^{-1} (Table 4). Different gas transfer models could explain our lower CH_4 fluxes compared to the literature. Our fluxes using the seagrass-derived k model from Dobashi and Ho (2022) were 2–11 times lower than other k models often used for the coastal or open ocean (Borges et al., 2004; Raymond & Cole, 2001; Wanninkhof, 2014). Seagrass meadows attenuate wave energy compared to bare sediment. Therefore, using coastal ocean gas transfer k models might overestimate the CH_4 emissions (Table 2). For example, Banerjee et al. (2018) and Ollivier et al. (2022) applied coastal ocean k model B04 and W14 models, respectively, which partially explains their higher CH_4 emissions.

Another reason for our relatively low CH_4 flux could be the lack of allochthonous CH_4 sources such as freshwater at our study site. Methane-enriched freshwater inputs could result in overestimates of CH_4 fluxes within seagrass meadows. The sea-air CH_4 fluxes from our sites and Australia (Ollivier et al., 2022; 10.6 µmol CH_4 m^{-2} d^{-1}) were at the lower end of published data (Table 4). Both studies were located in coastal bays with high salinity and limited tidal or freshwater influence. Our fluxes were two orders of magnitude lower than a brackish lagoon in India (120 µmol CH_4 m^{-2} d^{-1}), and a meso-tidal lagoon in Portugal (307 µmol CH_4 m^{-2} d^{-1}), France and US (Table 4; Al-Haj et al., 2022; Bahlmann et al., 2015; Banerjee et al., 2018). These other seagrass sites were in tidal systems with freshwater inputs suggesting that the reported high CH_4 fluxes could be partially explained by external freshwater or marsh inputs. CH_4 contribution from external sources has been observed in other tidally influenced ecosystems such as mangroves and saltmarshes where higher CH_4 concentration in porewater drives the high surface water CH_4 (Call et al., 2018; Santos et al., 2019; Yau et al., 2022). Flanking saltmarshes adjacent to seagrass export CH_4, elevating CH_4 flux in the seagrass meadows (Al-Haj et al., 2022). Since our system is not directly influenced by flanking marshes, porewater, and freshwater inputs, the relatively low CH_4 sea-air fluxes likely represent emissions from subtidal seagrass habitats.

We combined our results with the literature to re-evaluate global CH_4 emissions from seagrass meadows. It is important to differentiate between sediment-water and sea-air fluxes (Table 4). Fluxes from the benthic chamber and sediment core incubation only capture the CH_4 from sediment to water. They do not account for the exchange of CH_4 across the water-air interface or potential CH_4 oxidation in the water column (Asplund

21698961, 2023, 6, Downloaded from https://agupubs.onlinelibrary.wiley.com/doi/10.1029/2022JG007295 by Edith Cowan University, Wiley Online Library on [22/08/2023]. See the Terms and Conditions (https://onlinelibrary.wiley.com/terms-and-conditions) on Wiley Online Library for rules of use; OA articles are governed by the applicable Creative Commons License

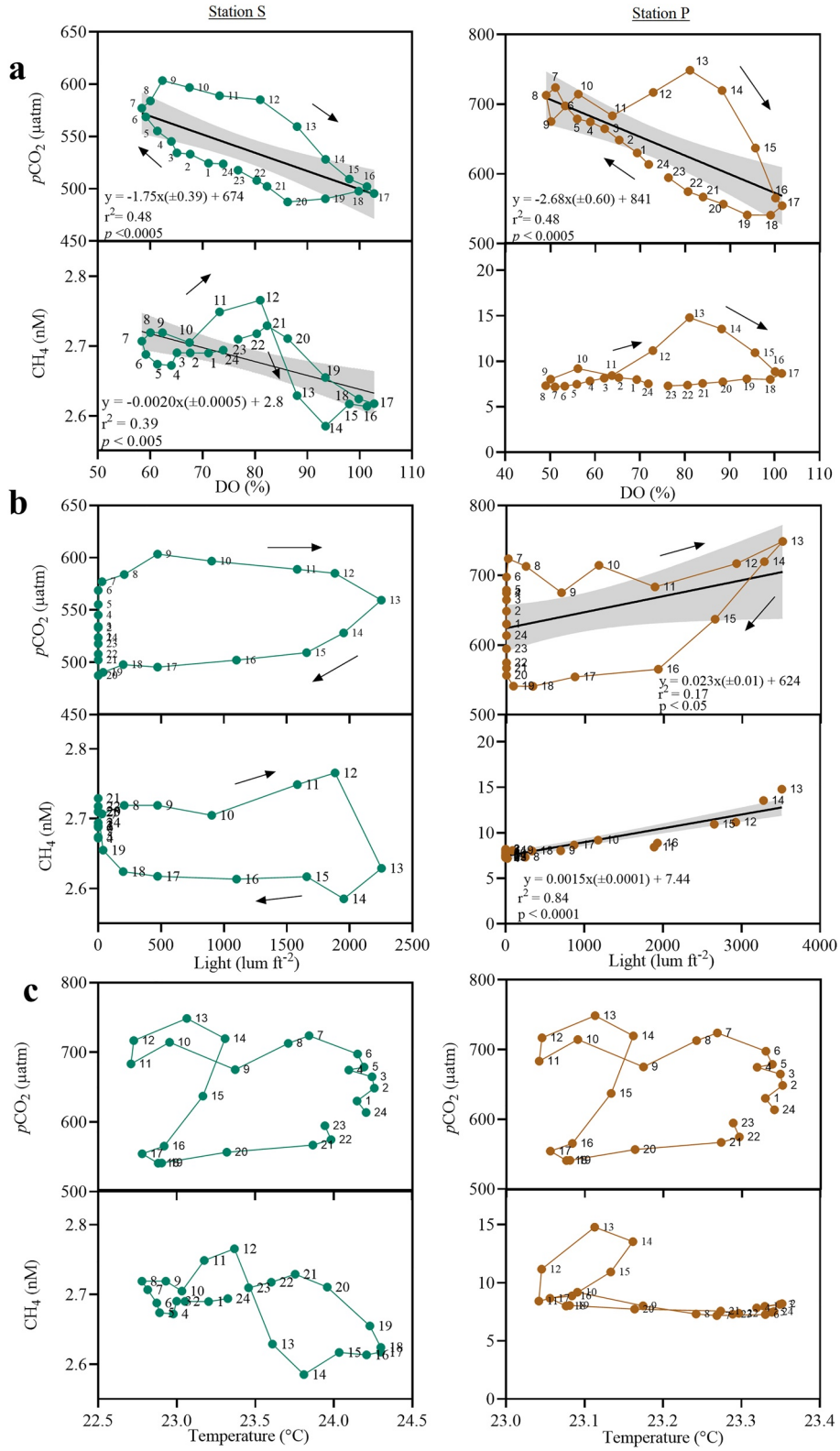

Figure 7. (a) Scatter plot of average hourly values of dissolved oxygen (DO), (b) light intensity, and (c) temperature against CH_4 and CO_2 in Station S (left) and Station P (right). The solid line represents the fitted regression equation (±SE), and the shaded area is the 95% confidence limits of the regression line, the r^2 value is the degree of correlation, and the p-value is the level of significance. The numbers inside the plots indicate the hour of the day. Arrows indicate the hysteresis pattern throughout the day.

21698961, 2023, 6, Downloaded from https://agupubs.onlinelibrary.wiley.com/doi/10.1029/2022JG007295 by Edith Cowan University, Wiley Online Library on [22/08/2023]. See the Terms and Conditions (https://onlinelibrary.wiley.com/terms-and-conditions) on Wiley Online Library for rules of use; OA articles are governed by the applicable Creative Commons License

Journal of Geophysical Research: Biogeosciences
10.1029/2022JG007295

Table 4
Mean of Methane (CH_4) in Sea-Air and Sediment-Water Fluxes in Seagrass Reported in the Literature

Location	Species	CH4 flux (μmol m^{-2} d^{-1})	Site	Method
Water-air				
Chilika Lagoon, India[a]	*Halodule sp. and Halophila sp*	120.0	Tidal lagoon	Water samples
Arcachon Lagoon, France[b]	*Z. noltii*	42.0	Tidal lagoon	Discrete water samples
Wallagoot, Australia[c]	*R. megacarpa*	33.8	Mouth of estuary	Continuous surface water
East Harbor, Massachusetts, USA[d]	*Z. marina*	107.5	Lagoon + marsh	Discrete water samples
Pleasant Bay, Massachusetts,USA[d]	*Z. marina*	113.8	Coastal lagoon	Discrete water samples
Swan Bay, Australia[e]	*Z. mulleri*	10.6	Tidal lagoon	Continuous surface water
Cadaques, Spain[f]	*P. oceanica*	0.1	Coastal bay	Continuous surface water
	Mean	**61.1 (±19.4)**		
	Geometric mean	**21.6**		
	Median	**42.0**		
Sediment-water				
Florida, USA[g]	*T. testudinum*	44.0	Coastal lagoon	Benthic chamber
Bimini, Bahamas[g]	*S. filiforme*	5.8	Coastal bay	Benthic chamber
Moreton Bay, Australia[h]	*Z. capricorni*	348.0	Coastal lagoon	Core incubation
Florida, USA[i]	*T. testudinum*	183.4	Coastal lagoon	Benthic chamber
Tomales Bay, USA[j]	*Z. marina*	35.7	Coastal inlet	Benthic chamber
Awerange Bay, Indonesia[k]	*E. acoroides*	95.7	Coastal bay	Benthic chamber
Arcachon Lagoon, France[b]	*Z. noltii*	98.4	Tidal lagoon	Water samples
Ria Formosa Lagoon, Portugal[l]	*Z. noltii*	307.2	Tidal lagoon	Core incubation
Red Sea, Saudi Arabia[m]	*H. uninervis*	48.1	Coastal inlet	Core incubation
Red Sea, Saudi Arabia[m]	*C. serrulata and H. uninervis*	401.3	Coastal inlet	Core incubation
Red Sea, Saudi Arabia[m]	*E. acoroides*	96.2	Coastal inlet	Core incubation
Red Sea, Saudi Arabia[m]	*T. ciliatum*	3.2	Coastal inlet	Core incubation
Red Sea, Saudi Arabia[m]	*H. decipiens*	1.4	Coastal inlet	Core incubation
Red Sea, Saudi Arabia[m]	*T. hemprichii*	6.5	Coastal inlet	Core incubation
Red Sea, Saudi Arabia[m]	*H. stipulacea and H. uninervis*	61.0	Coastal inlet	Core incubation
Chwaka Bay, Tanzania[n]	*T. hemprichii*	74.8	Coastal bay + mangrove	Benthic chamber
Red Sea, Saudi Arabia [o]	*H. stipulacea and H. unervis*	59.7	Coastal lagoon	Core incubation
Virginia, USA[p]	*Z.marina*	136.7	Coastal bay with marsh	Benthic chamber
Mediterranean Sea, Italy[q]	*P. oceanica*	106.0	Coastal bay	Core incubation
Wallis Lake, Australia[c]	*H. ovalis*	45.4	Mouth of estuary	Benthic chamber
Wallis Lake, Australia[c]	*P. australia*	279.3	Mouth of estuary	Benthic chamber
Wallis Lake, Australia[c]	*Z. muelleri*	46.0	Mouth of estuary	Benthic chamber
Wallis Lake, Australia[c]	*Z. muelleri*	10.9	Mouth of estuary	Benthic chamber

21698961, 2023, 6, Downloaded from https://agupubs.onlinelibrary.wiley.com/doi/10.1029/2022JG007295 by Edith Cowan University, Wiley Online Library on [22/08/2023]. See the Terms and Conditions (https://onlinelibrary.wiley.com/terms-and-conditions) on Wiley Online Library for rules of use; OA articles are governed by the applicable Creative Commons License

Table 4
Continued

Location	Species	CH4 flux (μmol m^{-2} d^{-1})	Site	Method
Finnland[r]	*Z. marina*	1.6	Coastal bay	Benthic chamber
Denmark[r]	*Z. marina*	3.4	Fjord and coastal bay	Benthic chamber
Sweden[r]	*Z. marina*	2.6	Coastal bay	Benthic chamber
East Harbor, Massachusetts, USA[d]	*Z. marina*	0.0	Back-barrier lagoon	Benthic chamber
Pleasant Bay, Massachusetts,USA[d]	*Z. marina*	73.3	Coastal lagoon	Benthic chamber
Cadaques, Spain[f]	*P. oceanica*	0.3	Coastal bay	Porewater samples
	Mean	**81.0 (±19.8)**		
	Geometric mean	**26.1**		
	Median	**47.1**		

Note. The mean (±SE), geometric mean, and median of sea-air and sediment-water CH_4 fluxes represent the global average.
[a]Banerjee et al. (2018). [b]Deborde et al. (2010). [c]Camillini (2020). [d]Al-Haj et al. (2022). [e]Ollivier et al. (2022). [f]This study. [g]Oremland (1975). [h]Moriarty et al. (1984). [i]Barber and Carlson (1993). [j]Sansone et al. (1998). [k]Alongi et al. (2008). [l]Bahlmann et al. (2015). [m]Garcias-Bonet (2017). [n]Lyimo et al. (2018). [o]Burkholz et al. (2020). [p]Oreska et al. (2020). [q]Schorn et al. (2022). [r]Asplund et al. (2022).

et al., 2022; Bonaglia et al., 2017; Schorn et al., 2022). Our measured sediment-water fluxes (0.25 μmol CH_4 m^{-2} d^{-1} in living seagrass) were up to two times higher than the sea-air CH_4 fluxes (0.11 μmol CH_4 m^{-2} d^{-1} at Station S), implying that sediment-water fluxes do not necessarily represent water-air fluxes. Earlier global estimates of seagrass CH_4 emissions to the atmosphere (1.25–401 μmol CH_4 m^{-2} d^{-1}) were extrapolated from studies using benthic chambers and sediment core incubations (Rosentreter et al., 2021). Therefore, we updated earlier compilations (Al-Haj et al., 2022) to differentiate between sea-air (8 sites) and sediment-water CH_4 (20 sites) fluxes in seagrass meadows (Table 4). Both sea-air and sediment-water CH_4 fluxes are highly variable. The geometric mean of sea-air and sediment-water CH_4 fluxes (21.6 and 26.1 μmol m^{-2} d^{-1}, respectively) was 3-fold lower than arithmetic mean values (61.6 ± 19.4 and 81.0 ± 19.8 μmol m^{-2} d^{-1}, respectively). The skewed data set suggests that geometric mean is likely a more realistic representation of fluxes (Williamson & Gattuso, 2022). Overall, previous compilations may have overestimated CH_4 emissions by relying on sediment-water fluxes and arithmetic mean values rather than sea-air and geometric mean values.

4.5. Implications for Carbon Sequestration

To evaluate the potential offset from carbon burial benefits, sea-air CH_4 fluxes were converted to CO_2-equivalents in 20 and 100 yr time horizons using SGWP of 96 and 45, respectively (Neubauer & Megonigal, 2015). The CO_2-equivalent emissions of CH_4 from Portilligat Bay were 0.05 and 0.03 g CO_2-eq m^2 yr^{-1} over 20 and 100 yr time horizons, respectively. The average carbon burial rates from surface 4 m thick seagrass *P. oceanica* matte are 142 ± 69 g CO_{2eq} m^{-2} yr^{-1} (Serrano et al., 2016). The estimated sea-air CH_4 emissions from *P. oceanica* offsets the average carbon burial from the surface matte only by <0.7% and <0.3% over a 20 and 100 yr time horizon, respectively. Yet, *P. oceanica* accumulates carbon over 6,000 yr (27,450 Mg CO_2-eq m^2; Lo Iacono et al., 2008; Mateo et al., 1997), a time scale much longer than the 9 yr CH_4 residence time in the atmosphere (Prather et al., 2012). Overall, the comparison of carbon burial in both the surface mat and the entire 6,000-yr-old mat provides an estimate of the small CH_4 offset compared to the strong carbon burial ability of *P. oceanica*. Our average CH_4/CO_2 flux ratio indicates that only about 0.01% of carbon mineralized is emitted as CH_4 and that CH_4 is likely to play a minor role offsetting carbon burial in this seagrass meadow (Figure 8).

Global sea-air CH_4 emissions upscaled from the total seagrass area of 160,387–266,562 km^2 were 1.3 (0.004–21.5) and 2.7 (0.009–45.9) Tg $CO_{2\text{-}eq}$ yr^{-1} in 100-yr and 20-yr time horizons, respectively. This estimation would offset only 1.6% and 3% (maximum of 25%) of global seagrass carbon burial in soils, which is estimated to be 138 ± 38 g C m^{-2} yr^{-1} (Table 5). Yet, global CH_4 SGWP estimates applied for static 20 and 100 time scales could not truly reflect the climatic impact of the seagrass habitat, given carbon storage over hundreds to thousands of years. Seagrass seems to emit less CH_4 than other coastal vegetated ecosystems such as mangroves and saltmarshes. For example, previous studies showed that methane emissions could offset <6% of carbon burial in a saltmarsh in China (Yau et al., 2022) and 18% in Australian mangroves receiving freshwater inputs (Rosentreter et al., 2018). Since seagrass are fully submerged and freshwater inputs are often limited, higher CH_4 oxidation in the water column could reduce CH_4 emissions relative to periodically inundated mangrove and saltmarsh systems. Overall, our study suggests that seagrass sequesters carbon without emitting large amounts of methane into the atmosphere.

5. Conclusion

Our continuous timeseries observations provide new insights into the spatial and diel patterns of CH_4 sediment-water and sea-air fluxes in seagrass-dominated ecosystems. Small CH_4 emissions to the atmosphere were measured in the coastal bay dominated by *P.oceanica*. Porewater profiles reflected methanogenesis activity in deep sediments. CH_4

21698961, 2023, 6, Downloaded from https://agupubs.onlinelibrary.wiley.com/doi/10.1029/2022JG007295 by Edith Cowan University, Wiley Online Library on [22/08/2023]. See the Terms and Conditions (https://onlinelibrary.wiley.com/terms-and-conditions) on Wiley Online Library for rules of use; OA articles are governed by the applicable Creative Commons License

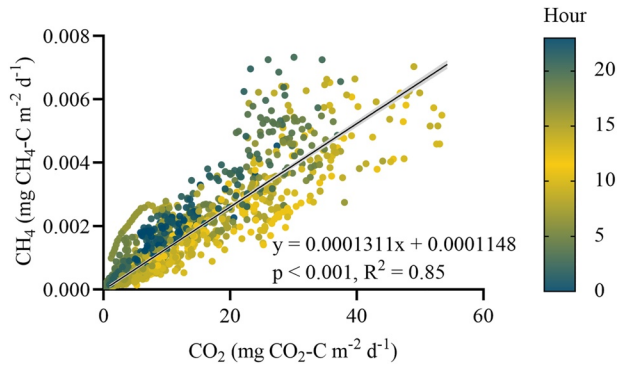

Figure 8. Relationship between CO_2 flux and CH_4 flux in Station S across the study period. The color represents hour of the day. The solid line represents the fitted regression equation (±SE), the shaded area is the 95% confidence limits of the regression line, the r^2 value and p-value is the degree of correlation and significance.

oxidation in the water column, supported by photosynthesis in seagrass, seems to explain the diel CH_4 pattern and low CH_4 emissions in the dense seagrass areas. Moreover, higher sediment-water fluxes than the sea-air fluxes in dense seagrass might imply that the sediment CH_4 could be the main CH_4 source. However, for the patchy seagrass, an opposite trend was observed. Lower sediment-water fluxes than the sea-air fluxes might imply there were additional CH_4 sources within the dead seagrass meadows. The high spatial variability of CH_4 within the bay highlights the importance of seagrass in regulating CH_4 emissions and/or the dilution by oceanic water. More continuous, high-resolution CH_4 measurements are required to decipher the causes of such contradictory CH_4 trends between dense and patchy seagrass sites, which could be linked to a combination of ocean water circulation, biological activity, or differences in porewater diffusive fluxes, among others.

Table 5
Global CH_4 Sea-Air and Sediment-Water Emissions Estimates From Seagrass and the Carbon Offset

Parameters			Air-sea	Sediment water
n			8	18
CH_4 flux	μmol CH_4 m^{-2} d^{-1}	Geomean[a]	30.1	26.1
	μmol CH_4 m^{-2} d^{-1}	Range	0.1–307.2	0.3–401.3
Area	km^2	Range		160,387–266,562[b]
Global CH_4 flux	Tg CH^4 yr^{-1}	Mean	0.03	0.02
	Tg CH^4 yr^{-1}	Range	0.00009–0.48	0.00028–0.62
$SGWP_{100}$	Tg $CO_{2\text{-eq}}$ yr-1	Mean	1.3	1.1
$SGWP_{20}$	Tg $CO_{2\text{-eq}}$ yr^{-1}	Mean	2.7	2.3
Carbon burial	g C m^{-2} yr^{-1}	Mean + SE	138 ± 38[c]	
	g C m^{-2} yr^{-1}	Range	45–190	
Global C burial	Tg C yr^{-1}	Mean + SE	22 ± 1	
Global C burial	Tg CO_2 yr^{-1}	Mean + SE	81 ± 4	
Offset of $SGWP_{100}$	%	Mean	1.6	1.4
	%	Range	0.02–11.6	0.05–15.1
Offset of $SGWP_{20}$	%	Mean	3.3	2.9
	%	Range	0.03–25	0.1–32

Note. The CH_4 flux for the seagrass is updated from Rosentreter, Al-Haj, Fulweiler, and Williamson (2021). *n* refers to number of study sites.

[a]Global geometric mean was calculated from the global complied data set based on Table 3. [b]Global seagrass area from McKenzie et al. (2020). [c]Global carbon burial was extracted from Mcleod et al. (2011).

21698961, 2023, 6, Downloaded from https://agupubs.onlinelibrary.wiley.com/doi/10.1029/2022JG007295 by Edith Cowan University, Wiley Online Library on [22/08/2023]. See the Terms and Conditions (https://onlinelibrary.wiley.com/terms-and-conditions) on Wiley Online Library for rules of use; OA articles are governed by the applicable Creative Commons License

Our study highlights the importance of differentiating sea-air and sediment-water flux when estimating seagrass CH_4 emissions. A low CH_4 offset to carbon burial was estimated both on local and global scale seagrass meadows. More site-specific carbon burial and long-term emission estimates are needed to resolve CH_4 dynamics in seagrass carbon budgets. The current evidence suggests the minor role of CH_4 emissions in offsetting seagrass carbon sequestration.

Data Availability Statement

Raw data are available in Zenodo (https://doi.org/10.5281/zenodo.7692274).

Acknowledgments
This project was funded by the Swedish Research Council (2020-00457) and Spanish RYC2019-027073-I project. OS was supported by I + D + i project PIE HOLOCENO 20213AT014 funded by MCIN/AEI/10.13039/501100011033 and FEDER. N. P-J. was supported by the Programme for Requalification of the Spanish University System 2021–2023 (Ministerio de Universidades), modality Margarita Salas Grants and financial support to CESAM (UIDB/50017/2020, UIDP/50017/2020, and LA/P/0094/2020; FCT/MCTES). We thank the locals from the Portlligat Bay for providing the boat.

References

Adyasari, D., Dimova, N. T., Dulai, H., Gilfedder, B. S., Cartwright, I., McKenzie, T., & Fuleky, P. (2023). Radon-222 as a groundwater discharge tracer to surface waters. *Earth-Science Reviews*, *238*, 104321. https://doi.org/10.1016/j.earscirev.2023.104321

Aleksandra, B.-G., & Katarzyna, Ł.-M. (2018). Porewater dissolved organic and inorganic carbon in relation to methane occurrence in sediments of the Gdańsk Basin (southern Baltic Sea). *Continental Shelf Research*, *168*, 11–20. https://doi.org/10.1016/j.csr.2018.08.008

Al-Haj, A. N., Chidsey, T., & Fulweiler, R. W. (2022). Two temperate seagrass meadows are negligible sources of methane and nitrous oxide. *Limnology and Oceanography*, *67*(S2), S193–S207. https://doi.org/10.1002/lno.12250

Al-Haj, A. N., & Fulweiler, R. W. (2020). A synthesis of methane emissions from shallow vegetated coastal ecosystems. *Global Change Biology*, *26*(5), 2988–3005. https://doi.org/10.1111/gcb.15046

Alongi, D., Trott, L., Undu, M., & Tirendi, F. (2008). Benthic microbial metabolism in seagrass meadows along a carbonate gradient in Sulawesi, Indonesia. *Aquatic Microbial Ecology*, *51*, 141–152. https://doi.org/10.3354/ame01191

Apostolaki, E. T., Caviglia, L., Santinelli, V., Cundy, A. B., Tramati, C. D., Mazzola, A., & Vizzini, S. (2022). The importance of dead seagrass (*Posidonia oceanica*) matte as a biogeochemical sink. *Frontiers in Marine Science*, *9*, 861998. https://doi.org/10.3389/fmars.2022.861998

Asplund, M. E., Bonaglia, S., Boström, C., Dahl, M., Deyanova, D., Gagnon, K., et al. (2022). Methane emissions from nordic seagrass meadow sediments. *Frontiers in Marine Science*, *8*, 811533. https://doi.org/10.3389/fmars.2021.811533

Bahlmann, E., Weinberg, I., Lavrič, J. V., Eckhardt, T., Michaelis, W., Santos, R., & Seifert, R. (2015). Tidal controls on trace gas dynamics in a seagrass meadow of the Ria Formosa lagoon (southern Portugal). *Biogeosciences*, *12*(6), 1683–1696. https://doi.org/10.5194/bg-12-1683-2015

Banerjee, K., Paneerselvam, A., Ramachandran, P., Ganguly, D., Singh, G., & Ramesh, R. (2018). Seagrass and macrophyte mediated CO_2 and CH_4 dynamics in shallow coastal waters. *PLoS One*, *13*(10), e0203922. https://doi.org/10.1371/journal.pone.0203922

Barber, T. R., & Carlson, P. R. (1993). Effects of seagrass die-off on benthic fluxes and porewater concentrations of $\sum CO_2$, $\sum H_2S$, and CH_4 in Florida bay sediments. In *Biogeochemistry of global change*. Springer. https://doi.org/10.1007/978-1-4615-2812-8_29

Bonaglia, S., Brüchert, V., Callac, N., Vicenzi, A., Chi Fru, E., & Nascimento, F. (2017). Methane fluxes from coastal sediments are enhanced by macrofauna. *Scientific Reports*, *13145*(1), 13145. https://doi.org/10.1038/s41598-017-13263-w

Borges, A. V., & Abril, G. (2011). Carbon dioxide and methane dynamics in estuaries. In *Treatise on estuarine and coastal science* (pp. 119–161). Elsevier. https://doi.org/10.1016/B978-0-12-374711-2.00504-0

Borges, A. V., Vanderborght, J.-P., Schiettecatte, L.-S., Gazeau, F., Ferrón-Smith, S., Delille, B., & Frankignoulle, M. (2004). Variability of the gas transfer velocity of CO_2 in a macrotidal estuary (the Scheldt). *Estuaries*, *27*(4), 593–603. https://doi.org/10.1007/BF02907647

Boudreau, B. P. (1997). *Diagenetic models and their implementation: Modeling transport and reactions in aquatic sediments*. Springer Berlin Heidelberg. Retrieved from http://catalog.hathitrust.org/api/volumes/oclc/35095947.html

Burkholz, C., Garcias-Bonet, N., & Duarte, C. M. (2020). Warming enhances carbon dioxide and methane fluxes from Red Sea seagrass (*Halophila stipulacea*) sediments. *Biogeosciences*, *17*(7), 1717–1730. https://doi.org/10.5194/bg-17-1717-2020

Call, M., Sanders, C. J., Enrich-Prast, A., Sanders, L., Marotta, H., Santos, I. R., & Maher, D. T. (2018). Radon-traced pore-water as a potential source of CO_2 and CH_4 to receding black and clear water environments in the Amazon Basin. *Limnology and Oceanography Letters*, *3*(5), 375–383. https://doi.org/10.1002/lol2.10089

Call, M., Santos, I. R., Dittmar, T., de Rezende, C. E., Asp, N. E., & Maher, D. T. (2019). High pore-water derived CO_2 and CH_4 emissions from a macro-tidal mangrove creek in the Amazon region. *Geochimica et Cosmochimica Acta*, *247*, 106–120. https://doi.org/10.1016/j.gca.2018.12.029

Camillini, N. (2020). *Carbon and nitrogen cycling in seagrass ecosystems*. [Southern Cross University; Application/pdf]. Retrieved from https://researchportal.scu.edu.au/esploro/outputs/doctoral/991012947400202368

Carnell, P. E., Ierodiaconou, D., Atwood, T. B., & Macreadie, P. I. (2020). Overgrazing of seagrass by sea urchins diminishes blue carbon stocks. *Ecosystems*, *23*(7), 1437–1448. https://doi.org/10.1007/s10021-020-00479-7

Chang, K.-Y., Riley, W., Crill, P., Grant, R., & Saleska, S. (2020). Hysteretic temperature sensitivity of wetland CH_4 fluxes explained by substrate availability and microbial activity. *Biogeosciences Discussions*, 1–38. https://doi.org/10.5194/bg-2020-177

Deborde, J., Anschutz, P., Guérin, F., Poirier, D., Marty, D., Boucher, G., et al. (2010). Methane sources, sinks and fluxes in a temperate tidal Lagoon: The Arcachon lagoon (SW France). *Estuarine, Coastal and Shelf Science*, *89*(4), 256–266. https://doi.org/10.1016/j.ecss.2010.07.013

Ding, W., Cai, Z., & Tsuruta, H. (2004). Diel variation in methane emissions from the stands of *Carex lasiocarpa* and *Deyeuxia angustifolia* in a cool temperate freshwater marsh. *Atmospheric Environment*, *38*(2), 181–188. https://doi.org/10.1016/j.atmosenv.2003.09.066

Dobashi, R., Ho, D. T. (2022). Air-sea gas exchange in a seagrass ecosystem, *Biogeochemistry: Air-Sea Exchange*

Duarte, C. M., Holmer, M., & Marbà, N. (2005). Plant-microbe interactions in seagrass meadows. In E. Kristensen, R. R. Haese, & J. E. Kostka (Eds.), *Coastal and estuarine studies* (Vol. 60, pp. 31–60). American Geophysical Union. https://doi.org/10.1029/CE060p0031

Duarte, C. M., & Krause-Jensen, D. (2017). Export from seagrass meadows contributes to marine carbon sequestration. *Frontiers in Marine Science*, *4*. https://doi.org/10.3389/fmars.2017.00013

Egger, M., Kraal, P., Jilbert, T., Sulu-Gambari, F., Sapart, C. J., Röckmann, T., & Slomp, C. P. (2016a). Anaerobic oxidation of methane alters sediment records of sulfur, iron, and phosphorus in the Black Sea. *Biogeosciences*, *13*(18), 5333–5355. https://doi.org/10.5194/bg-13-5333-2016

Egger, M., Lenstra, W., Jong, D., Meysman, F. J. R., Sapart, C. J., van der Veen, C., et al. (2016b). Rapid sediment accumulation results in high methane effluxes from coastal sediments. *PLoS One*, *11*(8), e0161609. https://doi.org/10.1371/journal.pone.0161609

21698961, 2023, 6, Downloaded from https://agupubs.onlinelibrary.wiley.com/doi/10.1029/2022JG007295 by Edith Cowan University, Wiley Online Library on [22/08/2023]. See the Terms and Conditions (https://onlinelibrary.wiley.com/terms-and-conditions) on Wiley Online Library for rules of use; OA articles are governed by the applicable Creative Commons License

Fourqurean, J. W., Duarte, C. M., Kennedy, H., Marbà, N., Holmer, M., Mateo, M. A., et al. (2012). Seagrass ecosystems as a globally significant carbon stock. *Nature Geoscience*, *5*(7), 505–509. https://doi.org/10.1038/ngeo1477

Froelich, P. N., Klinkhammer, G. P., Bender, M. L., Luedtke, N. A., Health, G. R., Cullen, D., et al. (1979). Early oxidation of organic matter in pelagic sediments of the eastern equatorial Atlantic: Suboxic diagenesis. *Geochimica et Cosmochimica Act*, *43*(7), 1075–1090. https://doi.org/10.1016/0016-7037(79)90095-4

Gacia, E., Duarte, C. M., & Middelburg, J. J. (2002). Carbon and nutrient deposition in a Mediterranean seagrass (*Posidonia oceanica*) meadow. *Limnology & Oceanography*, *47*(1), 23–32. https://doi.org/10.4319/lo.2002.47.1.0023

Garcias-Bonet, N., & Duarte, C. M. (2017). Methane production by seagrass ecosystems in the Red Sea. *Frontiers in Marine Science*, *4*, 10. https://doi.org/10.3389/fmars.2017.00340

Heiri, O., Lotter, A. F., & Lemcke, G. (2001). Loss on ignition as a method for estimating organic and carbonate content in sediments: Reproducibility and comparability of results. *Journal of Paleolimnology*, *25*(1), 101–110. https://doi.org/10.1023/a:1008119611481

Hilt, S., Grossart, H., McGinnis, D. F., & Keppler, F. (2022). Potential role of submerged macrophytes for oxic methane production in aquatic ecosystems. *Limnology and Oceanography*, *67*(S2), S76–S88. https://doi.org/10.1002/lno.12095

Hoehler, T. M., Borowski, W. S., Alperin, M. J., Rodriguez, N. M., & Paull, C. K. (2000). Model, stable isotope, and radiotracer characterization of anaerobic methane oxidation in gas hydrate-bearing sediments of the Blake ridge. In C. K. Paull, R. Matsumoto, P. J. Wallace, & W. P. Dillon (Eds.) *Proceedings of the Ocean Drilling Program, Scientific Results* (Vol. 164). https://doi.org/10.2973/odp.proc.sr.164.2000

Kaal, J., Serrano, O., del Río, J. C., & Rencoret, J. (2018). Radically different lignin composition in *Posidonia* species may link to differences in organic carbon sequestration capacity. *Organic Geochemistry*, *124*, 247–256. https://doi.org/10.1016/j.orggeochem.2018.07.017

Kennedy, H., Beggins, J., Duarte, C. M., Fourqurean, J. W., Holmer, M., Marbà, N., & Middelburg, J. J. (2010). Seagrass sediments as a global carbon sink: Isotopic constraints: Seagrass meadows as carbon sinks. *Global Biogeochemical Cycles*, *24*(4). https://doi.org/10.1029/2010GB003848

Knox, S. H., Bansal, S., McNicol, G., Schafer, K., Sturtevant, C., Ueyama, M., et al. (2021). Identifying dominant environmental predictors of freshwater wetland methane fluxes across diurnal to seasonal time scales. *Global Change Biology*, *27*(15), 3582–3604. https://doi.org/10.1111/gcb.15661

Lee, J.-M., & Kim, G. (2006). A simple and rapid method for analyzing radon in coastal and ground waters using a radon-in-air monitor. *Journal of Environmental Radioactivity*, *89*(3), 219–228. https://doi.org/10.1016/j.jenvrad.2006.05.006

Leiva-Dueñas, C., López-Merino, L., Serrano, O., Martínez Cortizas, A., & Mateo, M. A. (2018). Millennial-scale trends and controls in *Posidonia oceanica* (*L. Delile*) ecosystem productivity. *Global and Planetary Change*, *169*, 92–104. https://doi.org/10.1016/j.gloplacha.2018.07.011

Lengier, M., Szymczycha, B., Brodecka-Goluch, A., Kłostowska, Ż., & Kuliński, K. (2021). Benthic diffusive fluxes of organic and inorganic carbon, ammonium, and phosphates from deep water sediments of the Baltic Sea. *Oceanologia*, *63*(3), 370–384. https://doi.org/10.1016/j.oceano.2021.04.002

Lerman, A. (1979). *Geochemical processes water and sediment environment*. John Wiley and Sons.

Li, L., Jiang, Z., Wu, Y., He, J., Fang, Y., Lin, J., et al. (2021). Interspecific differences in root exudation for three tropical seagrasses and sediment pore-water dissolved organic carbon beneath them. *Marine Pollution Bulletin*, *8*, 113059. https://doi.org/10.1016/j.marpolbul.2021.113059

Li, Y., Fichot, C. G., Geng, L., Scarratt, M. G., & Xie, H. (2020). The contribution of methane photoproduction to the oceanic methane paradox. *Geophysical Research Letters*, *47*(14). https://doi.org/10.1029/2020GL088362

Lo Iacono, C., Mateo, M. A., Gràcia, E., Guasch, L., Carbonell, R., Serrano, L., et al. (2008). Very high-resolution seismo-acoustic imaging of seagrass meadows (Mediterranean Sea): Implications for carbon sink estimates. *Geophysical Research Letters*, *35*(18), L18601. https://doi.org/10.1029/2008GL034773

Lovelock, C. E., & Duarte, C. M. (2019). Dimensions of blue carbon and emerging perspectives. *Biology Letters*, *15*(3), 20180781. https://doi.org/10.1098/rsbl.2018.0781

Lyimo, L. D., Gullström, M., Lyimo, T. J., Deyanova, D., Dahl, M., Hamisi, M. I., & Björk, M. (2018). Shading and simulated grazing increase the sulfide pool and methane emission in a tropical seagrass meadow. *Marine Pollution Bulletin*, *134*, 89–93. https://doi.org/10.1016/j.marpolbul.2017.09.005

Majtényi-Hill, C., Reithmaier, G., Yau, Y. Y. Y., Serrano, O., Piñeiro-Juncal, N., & Santos, I. R. (2023). Inorganic carbon outwelling from a Mediterranean seagrass meadow using radium isotopes. *Estuarine, Coastal and Shelf Science*, *283*, 108248. https://doi.org/10.1016/j.ecss.2023.108248

Martens, C. S., & Klump, M. J. (1980). Biogeochemical cycling in an organic-rich coastal marine basin—I. Methane sediment-water exchange processes. *Geochimica et Cosmochimica Acta*, *44*(3), 471–490. https://doi.org/10.1016/0016-7037(80)90045-9

Mateo, M. A., Romero, J., Pérez, M., Littler, M. M., & Littler, D. S. (1997). Dynamics of millenary organic deposits resulting from the growth of the Mediterranean seagrass*Posidonia oceanica*. *Estuarine, Coastal and Shelf Science*, *44*(1), 103–110. https://doi.org/10.1006/ecss.1996.0116

McKenzie, L. J., Nordlund, L. M., Jones, B. L., Cullen-Unsworth, L. C., Roelfsema, C., & Unsworth, R. K. F. (2020). The global distribution of seagrass meadows. *Environmental Research Letters*, *15*(7), 074041. https://doi.org/10.1088/1748-9326/ab7d06

Mcleod, E., Chmura, G. L., Bouillon, S., Salm, R., Björk, M., Duarte, C. M., et al. (2011). A blueprint for blue carbon: Toward an improved understanding of the role of vegetated coastal habitats in sequestering CO_2. *Frontiers in Ecology and the Environment*, *9*(10), 552–560. https://doi.org/10.1890/110004

Moriarty, D. J. W., Boon, P. I., Hansen, J. A., Hunt, W. G., Poiner, I. R., Pollard, P. C., et al. (1984). Microbial biomass and productivity in seagrass beds. *Geomicrobiology Journal*, *4*(1), 21–51. https://doi.org/10.1080/01490458509385919

Murase, J., & Sugimoto, A. (2005). Inhibitory effect of light on methane oxidation in the pelagic water column of a mesotrophic lake (Lake Biwa, Japan). *Limnology & Oceanography*, *50*(4), 1339–1343. https://doi.org/10.4319/lo.2005.50.4.1339

Neubauer, S. C., & Megonigal, J. P. (2015). Moving beyond global warming potentials to quantify the climatic role of ecosystems. *Ecosystems*, *18*(6), 1000–1013. https://doi.org/10.1007/s10021-015-9879-4

Ollivier, Q. R., Maher, D. T., Pitfield, C., & Macreadie, P. I. (2022). Net drawdown of greenhouse gases (CO_2, CH_4, and N_2O) by a temperate Australian seagrass meadow. *Estuaries and Coasts*, *45*(7), 2026–2039. https://doi.org/10.1007/s12237-022-01068-8

Oremland, R. S. (1975). Methane production in shallow-water, tropical marine sediments. *Applied Microbiology*, *30*(4), 7–608. https://doi.org/10.1128/am.30.4.602-608.1975

Oreska, M. P. J., McGlathery, K. J., Aoki, L. R., Berger, A. C., Berg, P., & Mullins, L. (2020). The greenhouse gas offset potential from seagrass restoration. *Scientific Reports*, *10*(1), 7325. https://doi.org/10.1038/s41598-020-64094-1

Piñeiro-Juncal, N., Kaal, J., Moreira, J. C. F., Martínez Cortizas, A., Lambais, M. R., Otero, X. L., & Mateo, M. A. (2021). Cover loss in a seagrass *Posidonia oceanica* meadow accelerates soil organic matter turnover and alters soil prokaryotic communities. *Organic Geochemistry*, *151*, 104140. https://doi.org/10.1016/j.orggeochem.2020.104140

Piñeiro-Juncal, N., Mateo, M., Holmer, M., & Martínez-Cortizas, A. (2018). Potential microbial functional activity along a *Posidonia oceanica* soil profile. *Aquatic Microbial Ecology*, *81*(2), 189–200. https://doi.org/10.3354/ame01872

21698961, 2023, 6, Downloaded from https://agupubs.onlinelibrary.wiley.com/doi/10.1029/2022JG007295 by Edith Cowan University, Wiley Online Library on [22/08/2023]. See the Terms and Conditions (https://onlinelibrary.wiley.com/terms-and-conditions) on Wiley Online Library for rules of use; OA articles are governed by the applicable Creative Commons License

Prather, M. J., Holmes, C. D., & Hsu, J. (2012). Reactive greenhouse gas scenarios: Systematic exploration of uncertainties and the role of atmospheric chemistry. *Geophysical Research Letters*, *39*(9), 2012GL051440. https://doi.org/10.1029/2012GL051440

Raymond, P., & Cole, J. (2001). Gas exchange in rivers and estuaries: Choosing a gas transfer velocity. *Estuaries and Coasts*, *24*(2), 312–317. https://doi.org/10.2307/1352954

Rosentreter, J. A., Al-Haj, A. N., Fulweiler, R. W., & Williamson, P. (2021). Methane and nitrous oxide emissions complicate coastal blue carbon assessments. *Global Biogeochemical Cycles*, *35*(2). https://doi.org/10.1029/2020GB006858

Rosentreter, J. A., Borges, A. V., Deemer, B. R., Holgerson, M. A., Liu, S., Song, C., et al. (2021). Half of global methane emissions come from highly variable aquatic ecosystem sources. *Nature Geoscience*, *14*(4), 225–230. https://doi.org/10.1038/s41561-021-00715-2

Rosentreter, J. A., Maher, D. T., Erler, D. V., Murray, R. H., & Eyre, B. D. (2018). Methane emissions partially offset "blue carbon" burial in mangroves. *Science Advances*, *4*(6), eaao4985. https://doi.org/10.1126/sciadv.aao4985

Roth, F., Sun, X., Geibel, M. C., Prytherch, J., Brüchert, V., Bonaglia, S., et al. (2022). High spatiotemporal variability of methane concentrations challenges estimates of emissions across vegetated coastal ecosystems. *Global Change Biology*, *28*(14), 16177–24322. https://doi.org/10.1111/gcb.16177

Sansone, F. J., Rust, T. M., & Smith, S. V. (1998). Methane distribution and cycling in Tomales Bay, California. *Estuaries*, *21*(1), 66. https://doi.org/10.2307/1352547

Santos, I. R., Maher, D. T., Larkin, R., Webb, J. R., & Sanders, C. J. (2019). Carbon outwelling and outgassing versus burial in an estuarine tidal creek surrounded by mangrove and saltmarsh wetlands. *Limnology & Oceanography*, *64*(3), 996–1013. https://doi.org/10.1002/lno.11090

Schorn, S., Ahmerkamp, S., Bullock, E., Weber, M., Lott, C., Liebeke, M., et al. (2022). Diverse methylotrophic methanogenic archaea cause high methane emissions from seagrass meadows. *Proceedings of the National Academy of Sciences*, *119*(9), e2106628119. https://doi.org/10.1073/pnas.2106628119

Serrano, O., Almahasheer, H., Duarte, C. M., & Irigoien, X. (2018). Carbon stocks and accumulation rates in Red Sea seagrass meadows. *Scientific Reports*, *8*(1), 15037. https://doi.org/10.1038/s41598-018-33182-8

Serrano, O., Gómez-López, D. I., Sánchez-Valencia, L., Acosta-Chaparro, A., Navas-Camacho, R., González-Corredor, J., et al. (2021). Seagrass blue carbon stocks and sequestration rates in the Colombian Caribbean. *Scientific Reports*, *11*(1), 11067. https://doi.org/10.1038/s41598-021-90544-5

Serrano, O., Lavery, P. S., López-Merino, L., Ballesteros, E., & Mateo, M. A. (2016). Location and associated carbon storage of erosional escarpments of seagrass *Posidonia* mats. *Frontiers in Marine Science*, *3*. https://doi.org/10.3389/fmars.2016.00042

Serrano, O., Mateo, M. A., Renom, P., & Julià, R. (2012). Characterization of soils beneath a *Posidonia oceanica* meadow. *Geoderma*, *185–186*, 26–36. https://doi.org/10.1016/j.geoderma.2012.03.020

Sieczko, A. K., Duc, N. T., Schenk, J., Pajala, G., Rudberg, D., Sawakuchi, H. O., & Bastviken, D. (2020). Diel variability of methane emissions from lakes. *Proceedings of the National Academy of Sciences*, *117*(35), 21488–21494. https://doi.org/10.1073/pnas.2006024117

Telesca, L., Belluscio, A., Criscoli, A., Ardizzone, G., Apostolaki, E. T., Fraschetti, S., et al. (2015). Seagrass meadows (*Posidonia oceanica*) distribution and trajectories of change. *Scientific Reports*, *5*(1), 12505. https://doi.org/10.1038/srep12505

Van Dam, B., Polsenaere, P., Barreras-Apodaca, A., Lopes, C., Sanchez-Mejia, Z., Tokoro, T., et al. (2021). Global trends in air-water CO_2 exchange over seagrass meadows revealed by atmospheric eddy covariance. *Global Biogeochemical Cycles*, *35*(4). https://doi.org/10.1029/2020GB006848

Wanninkhof, R. (2014). Relationship between wind speed and gas exchange over the ocean revisited. *Limnology and Oceanography: Methods*, *12*(6), 351–362. https://doi.org/10.4319/lom.2014.12.351

Ward, B. B., Kilpatrick, K. A., Novellit, P. C., & Scrantont, M. I. (1987). Methane oxidation and methane fluxes in the ocean surface layer and deep anoxic waters. *Nature*, *4*(6119), 226–229. https://doi.org/10.1038/327226a0

Webb, J. R., Maher, D. T., & Santos, I. R. (2016). Automated, in situ measurements of dissolved CO_2, CH_4, and $\delta^{13}C$ values using cavity enhanced laser absorption spectrometry: Comparing response times of air-water equilibrators: Equilibrator measurement of dissolved CO_2, CH_4, and $\delta^{13}C$ values. *Limnology and Oceanography: Methods*, *14*(5), 323–337. https://doi.org/10.1002/lom3.10092

Weber, T., Wiseman, N. A., & Kock, A. (2019). Global ocean methane emissions dominated by shallow coastal waters. *Nature Communications*, *10*(1), 4584. https://doi.org/10.1038/s41467-019-12541-7

Weiss, R. F. (1974). Carbon dioxide in water and seawater: The solubility of a non-ideal gas. *Marine Chemistry*, *2*(3), 203–215. https://doi.org/10.1016/0304-4203(74)90015-2

Whiting, G. J., & Chanton, J. P. (1993). Primary production control of methane emission from wetlands. *Nature*, *364*(6440), 794–795. https://doi.org/10.1038/364794a0

Williamson, P., & Gattuso, J.-P. (2022). Carbon removal using coastal blue carbon ecosystems is uncertain and unreliable, with questionable climatic cost-effectiveness. *Frontiers in Climate*, *4*, 853666. https://doi.org/10.3389/fclim.2022.853666

Yamamoto, S., Alcauskas, J. B., & Crozier, T. E. (1976). Solubility of methane in distilled water and seawater. *Journal of Chemical & Engineering Data*, *21*(1), 78–80. https://doi.org/10.1021/je60068a029

21698961, 2023, 6, Downloaded from https://agupubs.onlinelibrary.wiley.com/doi/10.1029/2022JG007295 by Edith Cowan University, Wiley Online Library on [22/08/2023]. See the Terms and Conditions (https://onlinelibrary.wiley.com/terms-and-conditions) on Wiley Online Library for rules of use; OA articles are governed by the applicable Creative Commons License